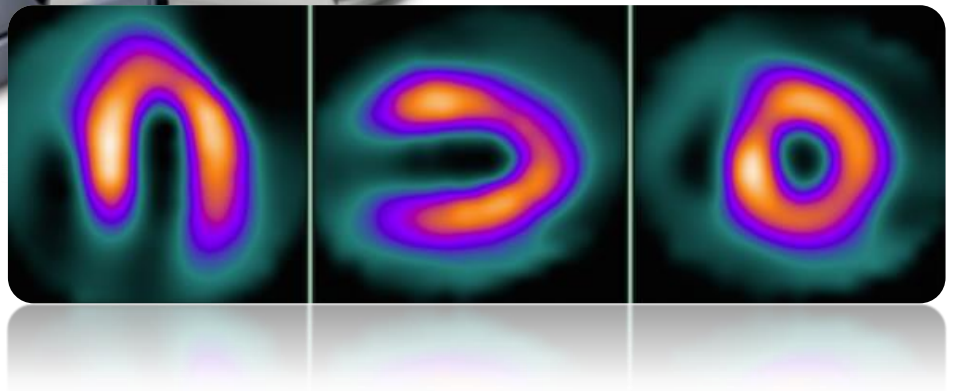


Optimization of myocardial blood flow quantification in Rubidium-82 PET myocardial perfusion imaging



13-09-2018
Author: S.S. Koenders, BSc
Technical Medicine, track Medical Imaging &
Interventions
University of Twente

Graduation committee:

Chairman: prof. dr. ir. C.H. Slump
Medical supervisors: dr. J.D. van Dijk, MSc. & prof. dr. P.L. Jager
Technical supervisor: prof. dr. ir. C.H. Slump
Process supervisor: N.S. Cramer Bornemann, MSc.
Extern member: prof. dr. R.H.J.A. Slart
Extra member: dr. J.A. van Dalen

Preface

Beste Lezer,

Voor u ligt de scriptie 'Optimization of myocardial blood flow quantification in Rubidium-82 PET myocardial perfusion imaging'. Het onderzoek is uitgevoerd op de afdeling Nucleaire Geneeskunde van Isala kliniek te Zwolle. Deze scriptie is geschreven in het kader van mijn afstuderen aan de opleiding Technical Medicine, richting Medical Imaging & Interventions, aan de universiteit van Twente. Van september 2017 tot en met juli 2018 ben ik bezig geweest met het onderzoek en het schrijven van de scriptie. Dit heb ik met veel plezier gedaan.

Door de intensieve begeleiding van mijn stagebegeleiders Joris van Dijk, Jorn van Dalen en Piet Jager en mijn begeleider vanuit de universiteit van Twente, Kees Slump, heb ik dit onderzoek tot een goed einde kunnen brengen. Hier ben ik hen erg dankbaar voor. Daarnaast wil ik mijn procesbegeleider, Nicole Cramer Bornemann, bedanken voor haar hulp gedurende mijn M2 stages en mijn afstuderen. Door je vragen omtrent mijn proces heb ik inzicht verkregen in mijn kwaliteiten en me kunnen ontwikkelen als Technisch Geneeskundige maar ook als persoon. Tevens wil ik Riemer Slart bedanken als buitenlid van mijn afstudeercommissie.

Verder wil ik graag alle andere collega's en Technische Geneeskunde studenten van de Nucleaire Geneeskunde en Cardiologie bedanken voor de gezellige tijd.

Ik hoop dat u met veel plezier mijn scriptie zult doorlezen.

Sabine Koenders

Zwolle, 30 juli 2018

Summary

Introduction: Cardiovascular disease is the second leading cause of death in the Netherlands. Of these cardiovascular deaths, 22% is due to coronary artery disease (CAD). Early detection and accurate diagnosis of CAD are essential. Myocardial blood flow (MBF) quantification using Rubidium-82 (Rb-82) in myocardial perfusion imaging (MPI) with positron emission tomography (PET) is increasing rapidly and is of added value in the diagnosis of CAD. MBF quantification provides valuable additional prognostic information. Further optimization of MBF quantification is required for more accurate MBF quantification and might offer the possibility for a “one-stop shop”. The aims were to 1) determine the impact of non-returning motion of the myocardium during pharmacological induced stress, called myocardial creep, on MBF quantification and 2) to derive and validate a temporal sampling protocol with a minimum number of time frames that still results in precise MBF quantification.

Myocardial creep

Method: Presence of myocardial creep was visually detected and corrected. Uncorrected and corrected MBFs for the left anterior descending (LAD), left circumflex (LCX) and right coronary artery (RCA) and the whole myocardium were compared. In addition, instructions on how to detect and correct for myocardial creep and an overview of software packages able to perform this correction were provided in a technical note.

Results: Myocardial creep was detected in 52% of the patients and significantly influenced the MBF values, especially in the RCA territory, as shown in Figure 1. In patients with myocardial creep, 83% had a change in MBF of >10% which is considered to possibly influence diagnostic interpretation. Only two of the four commonly used software packages to quantify MBF have the functionality to detect and correct for myocardial creep.

Conclusion: Detection and correction of myocardial creep seems necessary to obtain accurate MBFs using PET Rb-82 as it may influence diagnosis. It is therefore important that all vendors provide this functionality in their software.

Minimization of temporal sampling protocol

Method: A simulation tool was used to assess the influence of minimizing temporal sampling using varying protocols with 26 to 14 frames. Protocols were considered for validation if the SD of the relative differences, with 26 frames as reference, was $\leq 5\%$. Next, two accepted protocols were validated. Rest and stress MBFs were calculated and compared between the new and reference protocol in clinical practice. New protocols were considered for clinical adoption if the SD of the relative differences was $\leq 10\%$.

Results: Six of the nine tested temporal sampling protocols were considered to provide precise results. The protocols with 20 and 14 frames were validated in clinical practice. Both protocols were considered for clinical adoption as the SDs of the relative differences were $\leq 10\%$ for rest and stress global MBF (whole myocardium).

Conclusion: The choice of temporal sampling protocol influences MBF outcomes. The minimum number of time frames that can be considered for clinical adoption is 14 frames. This reduces reconstruction time and might provide the possibility for a “one-stop shop”.

Abbreviations

BMI	Body mass index
CAD	Coronary artery disease
CT	Computed tomography
EF	Ejection fraction
LAD	Left anterior descending
LCX	Left circumflex
LV	Left ventricle
MBF	Myocardial blood flow
MFR	Myocardial flow reserve
MPI	Myocardial perfusion imaging
PET	Positron emission tomography
Rb-82	Rubidium-82
RCA	Right coronary artery
ROI	Region of interest
SPECT	Single photon emission computed tomography
TAC	Time activity curve

Table of contents

Preface		i
Summary		iii
Abbreviations		v

Chapter 1	General introduction	1
Chapter 2	Impact of regadenoson induced myocardial creep on dynamic Rubidium-82 PET myocardial blood flow quantification	13
Chapter 3	How to detect and correct myocardial creep in myocardial perfusion imaging using Rubidium-82 PET?	27
Chapter 4	Simulation of myocardial blood flow quantification using the one-tissue compartment model provided in R	39
Chapter 5	Minimization of temporal sampling for myocardial blood flow quantification using Rubidium-82 PET	47
Chapter 6	Future perspectives and general conclusion	61

References		65
------------	--	----

Chapter 1

General introduction

Introduction

Cardiovascular disease is the second leading cause of death in the Netherlands [1]. Of these cardiovascular deaths, 22% is due to coronary artery disease (CAD) [1]. In patients with suspected CAD and an intermediate pre-probability, non-invasive testing is recommended [2]. Myocardial perfusion imaging (MPI) is a non-invasive imaging modality which has proven to be of added value in the diagnosis of CAD. MPI using Rubidium-82 (Rb-82) positron emission tomography (PET) provides the possibility to quantify the myocardial blood flow (MBF). MBF quantification provides valuable additional prognostic information about the extent and functional importance of possible stenosis [3–5]. MPI using Rb-82 PET can therefore play an important role in the early detection of CAD and detection of balanced 3-vessel disease. Moreover, of the non-invasive imaging modalities, PET remains the most accurate for MBF quantification [6].

To calculate MBF, dynamic images are required. These images are used to measure the activity distribution over time resulting in time activity curves (TACs). The TACs are used as input function for compartment analysis to calculate MBF. The one-tissue compartment model of Lortie et al. is most commonly used for this compartment analysis [7]. Besides MBF, myocardial flow reserve (MFR) can be calculated. The MFR represents the relative reserve of the coronary circulation and is the ratio between the MBF at maximal coronary vasodilation (MBF stress) and at rest (MBF rest) [6]. Gewirtz et al. showed that adding quantification of MFR improves risk assessment and can lead to reassignment of patients to other risk groups. This improves prognostic assessment which is important for the management of CAD [2]. It is important to differentiate between those patients with more severe forms of CAD and patients with a less severe form of disease. Patients with a severe form of disease may have an improvement in outcome with a more aggressive intervention such as revascularization. However, for patients with a less severe form of CAD it is important to avoid unnecessary invasive and non-invasive tests and revascularization procedures. Further optimization of MBF and MFR quantification might further increase diagnostic accuracy of CAD and thereby improve risk assessment.

There are several factors that affect MBF quantification which can be optimized. For example, the reconstruction method and settings, temporal sampling and motion [8]. Of these factors, reconstruction method and settings, is already further optimized after the implementation of MBF quantification in Isala hospital. We have shown that the use of Time of Flight (TOF) reconstructions, which takes almost two and half times longer than non-TOF reconstruction, could safely be replaced with non-TOF without hampering the MBF quantification [9]. This resulted in a decreased reconstruction time for the clinical routine.

Although the first optimization steps for the reconstruction method and settings are already taken, more steps concerning temporal sampling and motion can still be made to further optimize MBF quantification. Dynamic scans are reconstructed from list-mode data using several time frames. Both the length and the number of time frames of the used temporal sampling protocol influence measured TACs. The length of the time frames are crucial to capture the first pass phase (activity in the left ventricle (LV)) [10] and an increasing number of time frames imply time-consuming reconstructions. Optimization of the temporal sampling protocol can therefore result in accurate MBF quantification while further reducing reconstruction time. This might provide the possibility for a “one-stop shop”: a one-day protocol for the acquisition and reconstruction of the static, gated and dynamic images, MBF quantification and evaluation of the scans. Furthermore, in clinical practice we

frequently observe a non-returning motion of the myocardium during pharmacological induced stress, called myocardial creep. This motion may result in biased MBF measurements and may hamper diagnostic accuracy.

The aim of this thesis is to further optimize MBF quantification by determining the impact of myocardial creep on MBF quantification, and optimization of the temporal sampling of dynamic PET Rb-82 scans to reduce reconstruction time.

Background

Coronary artery disease

CAD is mainly caused by atherosclerosis [11]. Atherosclerosis is the build-up of plaque inside the artery walls. The coronary arteries that supply oxygenated blood to the myocardium (heart muscle) become narrowed due to this plaque build-up and this results in a poor blood flow to the myocardium. This decreased blood flow is called ischemia if the narrowing of the coronary arteries result in an inadequate oxygen supply to the myocardium. In case of present ischemia, there is an abnormal myocardial blood flow (MBF) during stress compared to the MBF during rest as illustrated in Figure 1. This results in a decreased myocardial flow reserve (MFR), the relative reserve of the coronary circulation, which is the ratio between MBF at stress and rest [6]. If CAD progresses and acute coronary syndrome (ACS) develops, there is also an abnormal MBF during rest [12]. If there is no pharmacologic or invasive intervention, ACS progresses to myocardial infarction, a discrete focus of ischemic muscle necrosis in the heart [13]. Therefore, early detection and accurate diagnosis and treatments of CAD are essential [14].

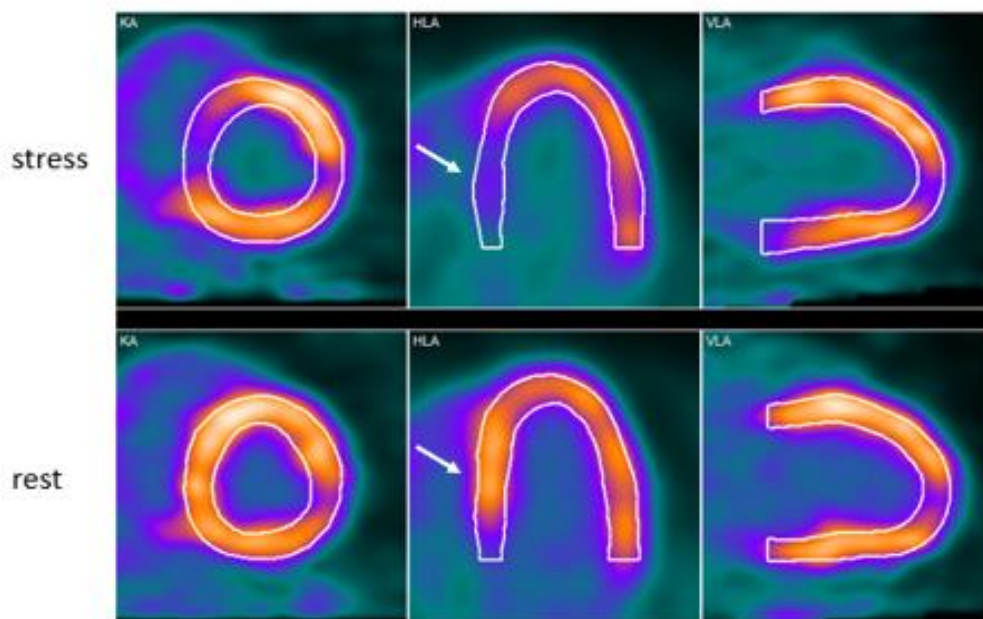


Figure 1: Tracer uptake during rest and stress PET MPI showing a decreased uptake during stress compared to rest indicating ischemia (arrow). From left to right for rest and stress: short axis view, horizontal long axis view and vertical long axis view.

Diagnostic testing

Non-invasive testing is recommended for patients with suspected CAD and an intermediate pre-probability [2]. There are several techniques for cardiac imaging. One of the techniques to image the anatomy of the three main coronary arteries, left anterior descending (LAD), left circumflex (LCX) and right coronary artery (RCA) as shown in Figure 2, is computed tomography (CT). CT can be used with coronary calcium scoring or after injection of iodinated contrast which is referred to as coronary computed tomography angiography (CCTA). Besides imaging the coronary anatomy, functional testing can be used to image the myocardial perfusion [2, 15]. Techniques that can image the myocardial perfusion are MPI using either single photon emission computed tomography (SPECT) or PET, cardiac magnetic resonance (CMR) imaging and stress echocardiography [2, 15]. An advantage of CMR and echocardiography is that they do not use ionizing radiation where PET and SPECT do [16]. The main drawback of stress echocardiography is the limited echogenicity of many patients and its operator-dependency [17]. Disadvantages of CMR include the contraindications of patients with non-MR-compatible implants or devices and patients with poor renal function due to the use of gadolinium-based contrast. Furthermore, the scan time of CMR is longer compared to PET and SPECT which is uncomfortable for patients [18]. The advantages of PET over SPECT are a better resolution and a lower radiation dose for the patient [19, 20]. Furthermore, PET has a higher diagnostic accuracy compared to SPECT [16]. Therefore, this thesis will focus on MPI PET and other imaging modalities will not further be discussed.

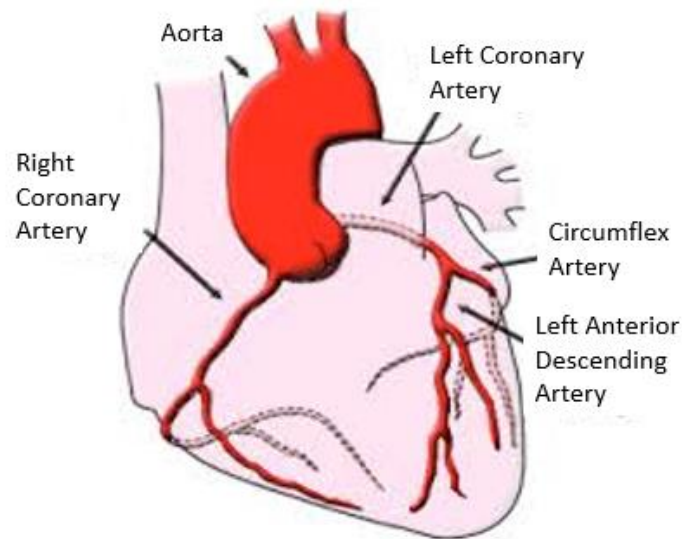


Figure 2: Overview of the three main coronary arteries: left anterior descending ((LAD), left circumflex (LCX) and right coronary artery (RCA)

MPI PET

PET imaging requires a tracer that emits positrons. When administered to the patient, the positron travels some distance in the tissue (range) after which it collides with an electron to annihilate and produce two 511 keV photons in opposite directions [21]. These photons are detected by the detector ring of the PET scanner which surrounds the patient. If two photons are detected almost simultaneously and 180° degrees apart, these detected counts are considered to be a positron annihilation along the path connecting the two detectors as illustrated in Figure 3A. Resolution of the PET system can be limited by a scattered coincidence: two photons are emitted less than 180° apart as illustrated in Figure 3B and by random coincidence as illustrated in Figure 3C [21]. Both have to be corrected for. A low-dose CT scan can be used for photon attenuation and scatter correction [19].

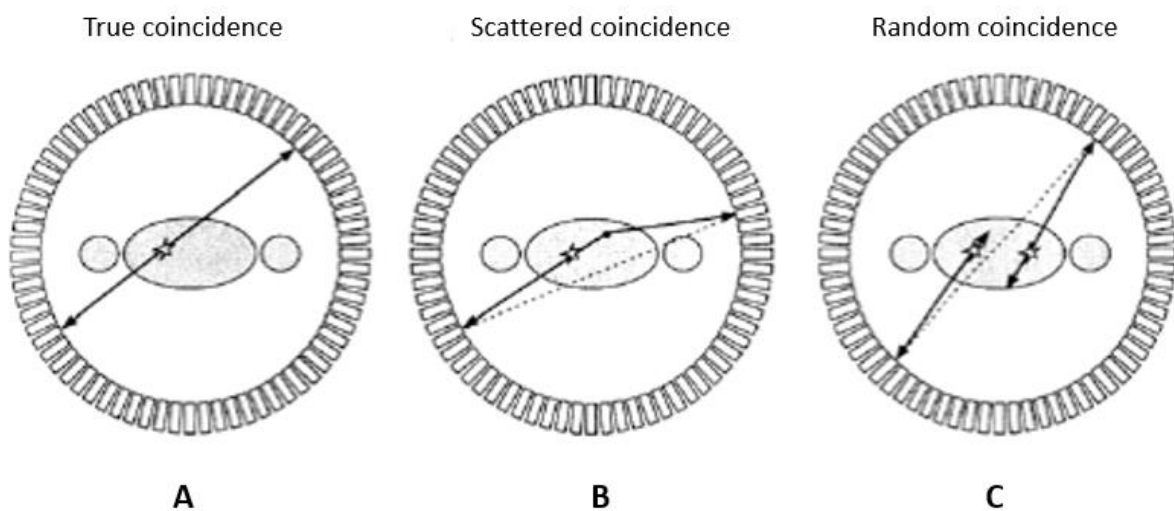


Figure 3: Besides true coincident detections (A), scattered (B) and random (C) detections can occur [21].

MPI PET using Rubidium-82

Several tracers are available for PET MPI of which currently Rb-82, ¹⁵O-water (¹⁵O) and ¹³N-ammonia (¹³N) are clinically the most widely used PET perfusion tracers with half-lives of 76 seconds, 2.06 minutes and 9.96 minutes, respectively [19, 22, 23]. However, widespread use of PET MPI is limited due to the need of an onsite or nearby cyclotron for ¹³N and ¹⁵O. The use of Rb-82 does not require a cyclotron but a generator and is therefore appealing [23]. To detect CAD, a Rb-82 PET imaging protocol comprises two scans, a rest and stress scan, as shown Figure 4. Stress is induced pharmacologically while the patient is lying in the scanner [24]. The three best known vasodilators are adenosine, dipyridamole and regadenoson. The latter is the first approved A_{2A} receptor agonist used as pharmacologic stress agent in MPI. Because regadenoson only stimulates A_{2A} receptors which causes the dilation of coronary vessels, side effects of regadenoson are experienced less intense and short in duration compared to adenosine and dipyridamole which also stimulates A_1 , A_{2B} and A_3 receptors [25–30].

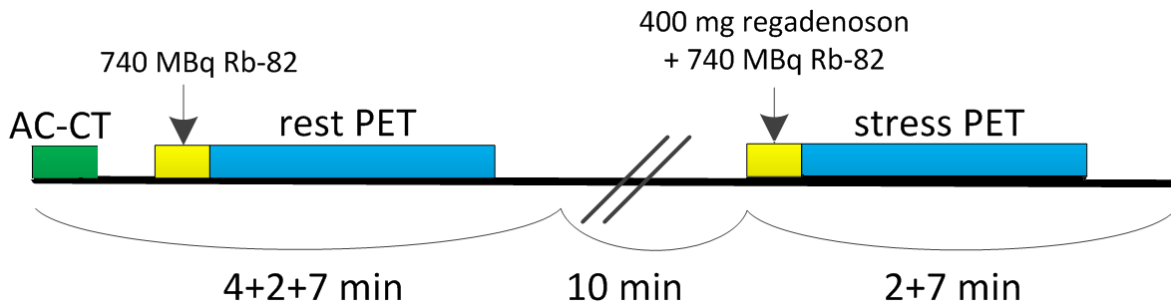


Figure 4: Example of an imaging protocol consisting of an attenuation CT followed by Rubidium-82 (Rb-82) administration for the rest scan. Ten minutes after the rest scan, again Rb-82 is administered intravenously after which regadenoson is administered to induce stress for the stress scan. Both scans take 7 minutes.

MBF quantification

Besides visualizing the relative rest and stress tracer uptake, Rb-82 PET has the possibility to quantify rest and stress MBF. MBF quantification using PET Rb-82 is shown to be accurate for detection and localization of CAD [3–5]. Hence, MBF quantification is proven to have an important added clinical value [8]. To quantify MBF, tracer distribution has to be estimated in units of blood flow per myocardial mass over time (mL/min/g) [15, 31]. To measure tracer distribution over time, a dynamic PET scan is acquired after administration of the activity after which several images are reconstructed using different time frames, as illustrated in Figure 5 [10]. To calculate the MBF for the whole myocardium or a specific region, the activity concentrations over time in the corresponding myocardial area and the LV (first pass phase) can be measured using regions of interest (ROIs) as shown in Figure 6. This is done for both the rest and stress scan. The myocardium contour is drawn, based on all data acquired during the tissue phase where a steady state is reached, i.e. data acquired >2:15 minutes after Rb-82 administration [32], as the activity is then primarily present in the myocardium. Next, these ROIs of the myocardium and LV are sampled in the reconstructed dynamic time frames to calculate time activity curves, as shown in Figure 7 [24].

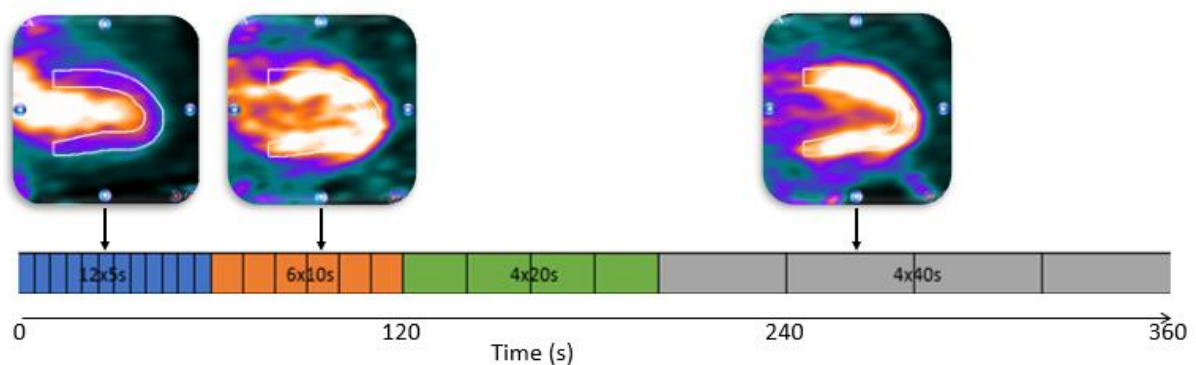


Figure 5: The temporal sampling protocol shown is the currently used protocol with 26 time frames. For each of the 26 time frames, individual images are reconstructed and combined into a dynamic series. Three phases can be distinguished: the first pass phase i.e. filling of the left ventricle (LV), intermediate phase (activity in LV and myocardium) and the tissue phase (activity in myocardium).

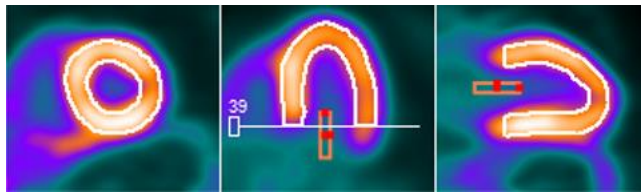


Figure 6: From left to right the short axis, horizontal long axis and vertical long axis view of the myocardium. An ROI is placed on the mitral valve and a myocardium contour is drawn to measure the activity concentration over time in the left ventricle (first pass phase) and the myocardium.

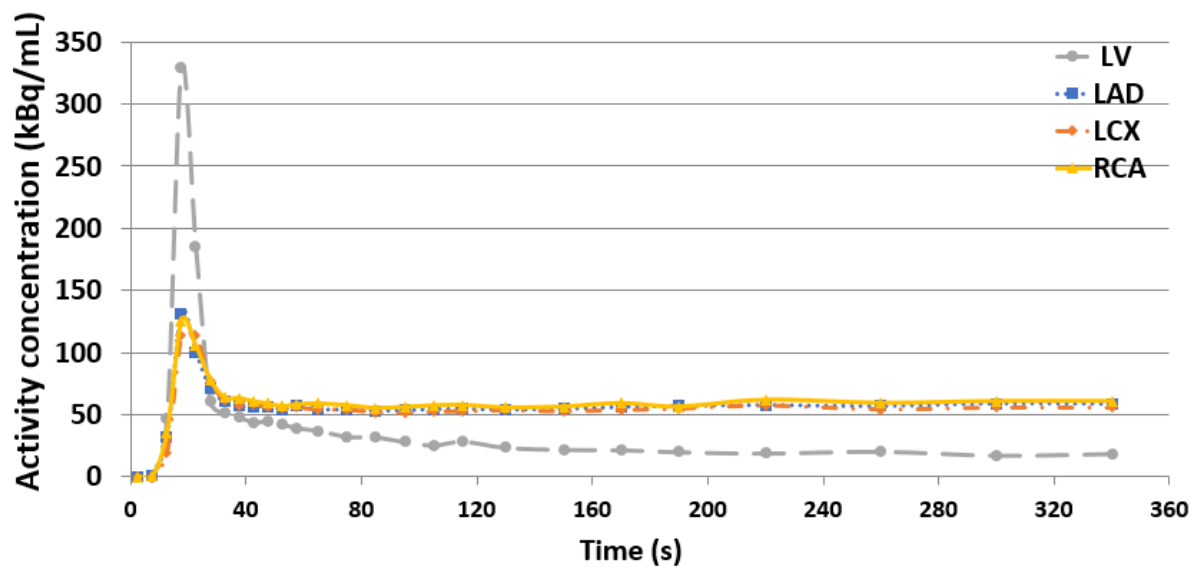


Figure 7: Time activity curves (TACs) showing the first pass phase where there is a peak for the left ventricle (LV) followed by the tissue phase where a steady state is reached for the three vascular territories: left anterior descending (LAD), left circumflex (LCX) and right coronary artery (RCA).

The first pass phase is generally sampled with small frame durations of five to ten seconds to assure sufficient temporal resolution and prevent under-sampling of the LV TAC [33–36]. The most common regions are those supplied by blood by one of the three main coronary arteries: LAD, LCX and RCA. The calculated TACs are then used as input function for compartmental analysis of which the one-tissue compartment model of Lortie et al. is most commonly used. First, K_1 and k_2 are calculated by fitting the model to the TACs [10]. K_1 is the tracer uptake from the blood pool to the myocardium and k_2 is the washout of tracer from the myocardium back into the blood pool as shown in Figure 8. To calculate the MBF out of these parameters, several correction factors have to be applied [10]. First, the extraction fraction needs to be corrected for as Rb-82 does not accumulate in the myocardium linearly proportional to perfusion. When one does not correct for this, the MBF will be underestimated with increasing MBF. Secondly, the partial volume effects, originated due to the limited resolution of PET systems, should be corrected. The partial volume effect is the loss of apparent activity in small regions or on edges, in particular due to the large positron range of Rb-82 and cardiac and respiratory motion. Lastly, one must correct for the spillover effects. Due to spillover, activity can already be observed in the edges of the myocardium during the first pass phase while the much lower uptake in the myocardium compared to the LV in this phase results in a gain of apparent activity in small regions or edges. If the spillover effect remains uncorrected, MBF quantification will be affected [37, 38]. The calculated rest and stress MBF, after the applied corrections, can be used to calculate the MFR. The MFR is the ratio of MBF during stress to MBF at rest ($MBF_{\text{Stress}}/MBF_{\text{rest}}$).

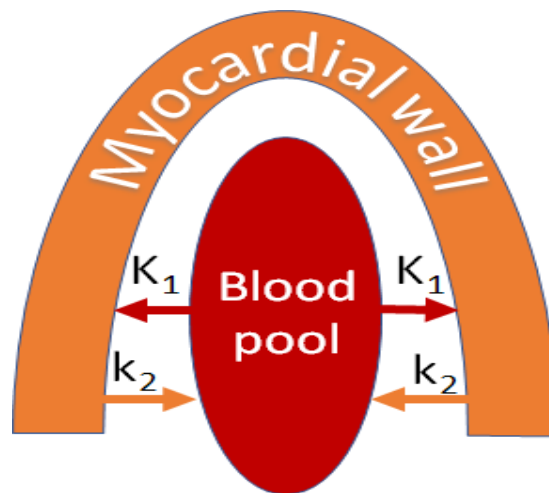


Figure 8: Schematic representation of a one-tissue compartment model with the blood pool as arterial input, the myocardial wall as compartment, K_1 explaining the tracer uptake in the myocardial wall and k_2 the washout from the myocardial wall to the blood [10].

Thesis outline

The aim of this thesis was to further optimize MBF quantification in Rb-82 PET MPI. For this purpose, we determined the impact of myocardial creep detection and correction on MBF quantification and minimized the temporal sampling protocol for the reconstruction of the dynamic images.

Chapter 2 of this thesis covers the presence of myocardial creep during pharmacological induced stress Rb-82 PET using regadenoson and its effect on MBF quantification. In **Chapter 3** instructions on how to detect and correct for this myocardial creep in MPI using Rb-82 PET are described. For further optimization of the reconstruction method, we focused on the temporal sampling protocol with the goal to minimize the number of time frames. Before we could test our hypothesis for minimization of temporal sampling, we assessed a method for simulation of MBF measurements which is described in **Chapter 4**. In **Chapter 5**, we sought to define the temporal sampling protocol with the minimal number of time frames still resulting in precise MBF measurements. In **Chapter 6** we discussed future perspectives including the clinical implications and the general conclusion

Chapter 2

Impact of regadenoson induced myocardial creep on dynamic Rubidium-82 PET myocardial blood flow quantification

J. Nucl. Cardiol. 2018

(in press)

Authors

S.S. Koenders, BSc^{1,4}, J.D. van Dijk, MSc, PhD¹, P.L. Jager, MD, PhD¹, J.P. Ottervanger, MD, PhD³, C.H. Slump, PhD⁴, J.A. van Dalen, PhD²

Isala hospital, Department of ¹Nuclear Medicine, ²Medical Physics, ³Cardiology, Zwolle, the Netherlands and ⁴MIRA: Institute for Biomedical Technology and Technical Medicine, University of Twente, Enschede, the Netherlands

Abstract

Background: Repositioning of the heart during myocardial perfusion imaging (MPI) using Rubidium-82 (Rb-82) PET may occur when using regadenoson. Our aim was to determine the prevalence and effect of correcting for this myocardial creep on myocardial blood flow (MBF) quantification.

Methods: We retrospectively included 119 consecutive patients who underwent dynamic rest and regadenoson induced stress MPI using Rb-82 PET. Presence of myocardial creep was visually assessed in the dynamic stress PET series by identifying differences between the automatically drawn myocardium contour and the activity. Uncorrected and corrected stress MBFs were compared for the three vascular territories (LAD, LCX, RCA) and for the whole myocardium.

Results: Myocardial creep was observed in 52% of the patients during stress. Mean MBF values decreased after correction in the RCA from 4.0 to 2.7 mL/min/g ($p<0.001$), in the whole myocardium from 2.7 to 2.6 mL/min/g ($p=0.01$) and increased in the LAD from 2.5 to 2.6 mL/min/g ($p=0.03$) and remained comparable in the LCX ($p=0.3$).

Conclusions: Myocardial creep is a frequent phenomenon when performing regadenoson induced stress Rb-82 PET and has a significant impact on MBF values, especially in the RCA territory. As this may hamper diagnostic accuracy, myocardial creep correction seems necessary for reliable quantification.

Introduction

The use of myocardial blood flow (MBF) quantification using Rubidium-82 (Rb-82) in myocardial perfusion imaging (MPI) with positron emission tomography (PET) is increasing rapidly [31, 39, 40]. MPI using Rb-82 PET is of added value in the diagnosis of coronary artery disease and the MBF quantification provides valuable additional prognostic information about the extent and functional importance of possible stenosis [3–5].

A dynamic PET acquisition including the capture of the first-pass bolus of the activity is required for MBF quantification. Pharmacological vasodilators are generally used to induce stress while the patient is lying inside the PET scanner [31, 41]. The three commonly used vasodilators are adenosine, dipyridamole and regadenoson. Due to the stimulation of A_1 , A_{2B} and A_3 receptors, adenosine and dipyridamole are associated with undesirable short-term side-effects as general discomfort, chest pain and hypotension and more severe side-effects such as atrioventricular block or bronchospasm [42, 43]. An alternative is regadenoson which is a more selective vasodilator that only stimulates A_{2A} receptors and is fast and better tolerated by patients [25–30]. Regadenoson has shown to result in accurate calculation of quantitative MBF values in MPI using Rb-82 PET with similar accuracy as compared to adenosine or dipyridamole [25, 27, 44–46]. An additional advantage of regadenoson is the significantly lower degree of patient motion as compared to adenosine, which can significantly affect the MBF quantification [35, 47–50].

Despite the reduced patient motion when using regadenoson, in clinical practice we frequently observe repositioning of the heart after administration of regadenoson. This so-called myocardial creep is presumably caused by an increasing respiration and lung volume and thereby repositioning of the diaphragm and heart after induction of pharmacological stress [51]. This motion may result in biased MBF measurements and may hamper diagnostic accuracy. Our aim was to determine the percentage of patients with this myocardial creep and to determine its effect on MBF values before and after correction in patients undergoing Rb-82 PET.

Methods

Study design

We retrospectively included 119 consecutive patients referred for MPI using Rb-82 PET/CT (GE Discovery 690, GE Healthcare) who underwent dynamic rest and pharmacological induced stress using regadenoson. This study was retrospective and approval by the medical ethics committee was therefore not required according to Dutch law. Nevertheless, all patients provided written informed consent for the use of data for research purposes.

Patient preparation and data acquisition

All subjects were asked to abstain from caffeine-containing substances for 24 hours and to discontinue dipyridamole containing medication for 48 hours before imaging. Prior to MPI, a low-dose CT scan was acquired during free-breathing to provide an attenuation map of the chest. This scan was made using a 5 mm slice thickness, 0.8 s rotation time, pitch of 0.97, collimation of 32x0.625 mm, tube voltage of 120 kV and tube current of 10 mA. Next, 740 MBq Rb-82 was

administered intravenously with a flow rate of 50 mL/min using a Sr-82/Rb-82 generator (CardioGen-82, Bracco Diagnostics Inc.). After the first elution, we induced pharmacological stress by administering 400 µg (5 mL) of regadenoson over 10 seconds. After a 5 mL saline flush (NaCl 0.9%) we administered a second dose of 740 MBq Rb-82. We acquired seven minute PET list-mode acquisitions after both Rb-82 administrations. Attenuation correction was applied to all data on the PET system after semi-automatic registration of CT and PET data. We reconstructed the dynamic data sets using 26 time frames (12x5 s, 6x10 s, 4x20 s and 4x40 s) with default settings as recommended by the manufacturer using 3D iterative reconstruction using 2 iterations and 24 subsets, while correcting for decay, attenuation, scatter and random coincidences, and dead time effects. Neither time-of-flight information, nor a post-processing filter or resolution modelling was used. Static images were reconstructed from 2:30 to 7:00 minutes for both rest and stress scans.

Data processing

The reconstructed dynamic images were processed using Corridor4DM software (v2015.02.64). Myocardium contours were automatically detected in both rest and stress scans based on the static images. Furthermore, a region of interest (ROI) was manually placed at the location of the mitral valve to estimate the activity in the blood pool (left ventricle). The activity concentrations in the myocardium contour and ROI were measured in the 26 reconstructed time frames to calculate the time activity curves (TACs) for the left ventricle (LV), for the three vascular territories: left anterior descending (LAD), left circumflex (LCX) and right coronary (RCA) artery and for the whole myocardium. The one-tissue compartment model of Lortie et al. based on a ROI methodology was used to calculate the MBF from the TACs using Corridor4DM [7].

The activity in the myocardium was visually compared with the drawn contours in all individual time frames to detect possible patient motion or myocardial creep. Myocardial creep was defined as gradual decreasing misalignment of the drawn myocardium contour with the activity present in the ventricle and/or myocardium, primarily in the inferior direction. This misalignment was at least one third of the width of the left ventricular myocardial wall and present in at least 2 time frames of which one had to include the first pass phase: the filling of the LV. If myocardial creep was present, manual re-alignment of the contour to the activity in the myocardium was applied in each of the related time frames. Motion not fulfilling the requirements of myocardial creep, suggesting general patient motion, was manually corrected by re-aligning the myocardium contour to the activity. Patients were excluded when patient motion was present together with myocardial creep to prevent biased results due to overlapping motion. Furthermore, patients with an unreliable TAC were also excluded. Unreliable TACs were defined as TACs showing no clear LV peak [10].

To evaluate the influence of myocardial creep correction, both rest and stress MBFs were calculated for the original data and for corrected data regarding the three vascular territories (LAD, LCX, RCA) and for the whole myocardium. Furthermore, the myocardial flow reserve (MFR), defined as the stress MBF divided by the rest MBF was calculated as well. A difference in MBF or MFR >10% between the corrected and uncorrected scans was considered to possibly influence diagnostic interpretation.

Statistical analysis

Patient-specific parameters and characteristics were determined as percentage or mean \pm standard deviation (SD) and compared with Chi-square and t-tests as appropriate, using SPSS Statistics version

22.0 (IBM Corporation). The MBF and MFR of the uncorrected and corrected data were compared using the Wilcoxon signed rank test. The level of statistical significance was set to 0.05 for all statistical analyses.

Results

Of the 119 patients, 11 (9%) were excluded due to the presence of both patient motion and myocardial creep in the stress data. An additional four patients (3%) were excluded due to unreliable TACs. An example of an unreliable TAC is shown in Figure 1. Of the remaining 104 patients, four (3%) showed only general patient motion in stress.

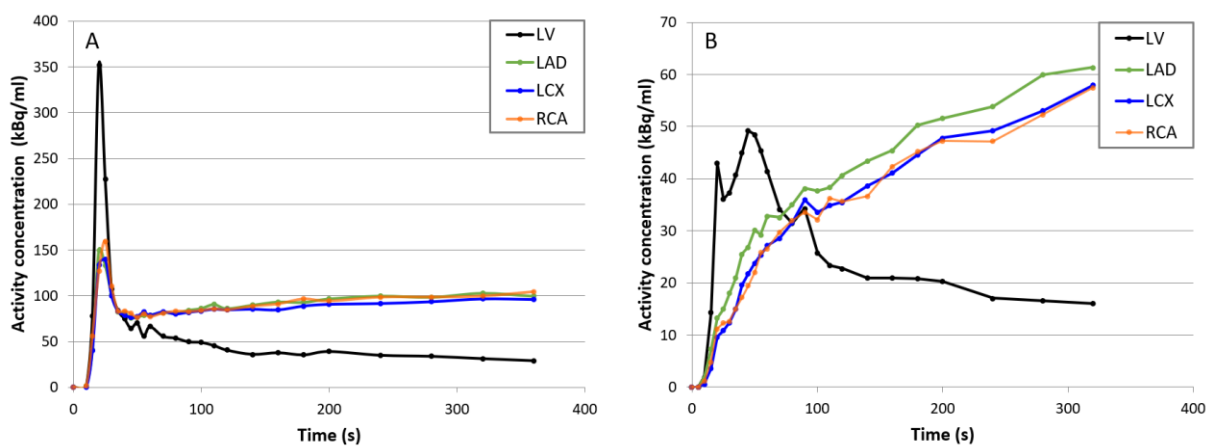


Figure 1: Linegraph showing (A) normal time activity curves (TACs) with a high peak value for the left ventricle (LV) during the first pass phase and where the vascular territories (LAD, LCX and RCA) gradually reach a steady state and (B) unreliable TACs with no clear LV peak and lack of steady state for the three vascular territories.

The baseline characteristics of the remaining 104 patients are summarized in Table 1. 54 (52%) Patients showed a myocardial creep during the stress scan, as illustrated in Figure 2. Patients with and without myocardial creep did not differ regarding gender, weight, body mass index (BMI), cardiac risk factors and scan outcomes ($p \geq 0.10$). Yet patients with myocardial creep were younger (64 years old) than patients without myocardial creep (70 years old, $p = 0.004$). Of the 54 patients with myocardial creep during stress, two patients also showed myocardial creep during the rest scan.

Table 1: Baseline characteristics and scan outcomes of all included patients (n=104) who underwent clinically indicated Rb-82 PET MPI.

	Patients with myocardial creep (n=54)	Patients without myocardial creep (n=50)	p Values (t-test / χ^2)
Age (years)	64 ± 11	70 ± 11	0.004
Male gender (%)	67	64	0.78
Weight (kg)	90 ± 15	85 ± 18	0.17
Length (cm)	175 ± 9	173 ± 10	0.32
BMI (kg/m ²)	29.3 ± 4.1	28.5 ± 5.8	0.44
Current smoker (%)	30	16	0.10
Hypertension (%)	46	50	0.71
Diabetes (%)	17	20	0.66
Dyslipidemia (%)	56	50	0.57
Family history (%)	69	54	0.13
Normal MPI scan (%)	76	64	0.18
Ischemic defects on MPI (%)	17	28	0.29
Non-reversible defects on MPI (%)	9	16	0.61

Data are presented as mean ± SD or as percentage.

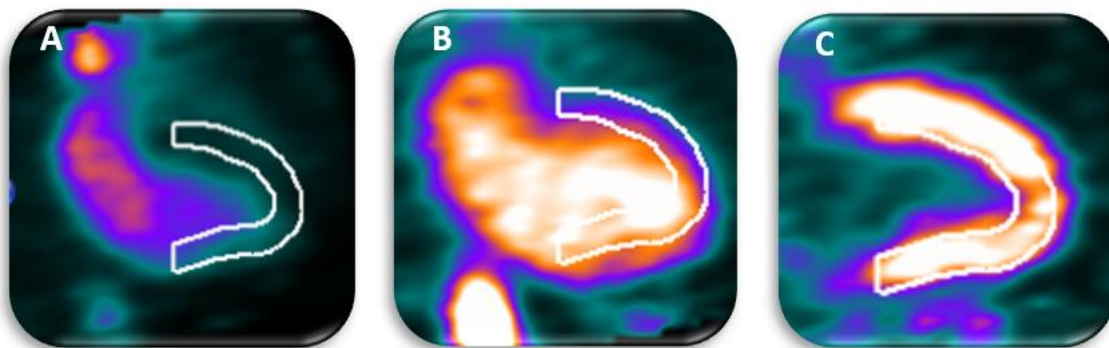


Figure 2: Example of a dynamic Rb-82 PET scan showing myocardial creep. In A (15-19s after injection), the activity reaches the LV and a misalignment of the automatically drawn myocardium contour and the activity is observed. In B (25-29s after injection), the activity has reached the left ventricle and the myocardium but the misalignment of the drawn myocardium contour and the activity is still observed. In C (360-420s after injection), activity is only present in the myocardium and the heart has returned to its original position resulting in alignment of the observed activity and myocardium contour.

The uncorrected and corrected MBF and MFR measurements, in both rest and stress, for each of the 3 territorial segments and for the myocardium as a whole (global result) are shown in Table 2 and Figure 3. When comparing the uncorrected and corrected data the largest differences were found for the RCA territory where the mean MBF decreased from 4.0 to 2.7 mL/min/g ($p < 0.001$) and the mean MFR from 3.5 to 2.4 ($p < 0.001$). Moreover, the MBF of the RCA decreased in 91% (49/54) of the patients and the MFR of the RCA decreased in 89% (48/54) of the patients, as shown in Figure 3D.

Furthermore, differences in MBF and MFR were found for the LAD territory and for the whole myocardium. The mean MBF increased for the LAD from 2.5 to 2.6 mL/min/g ($p=0.03$) and for the MFR from 2.2 to 2.3 ($p=0.006$) and for the whole myocardium the mean MBF and MFR values decreased from 2.7 to 2.6 mL/min/g ($p=0.01$) and from 2.4 to 2.3 ($p=0.03$), respectively. No significant differences were found for the LCX territory in stress ($p=0.3$) nor in the rest scans ($p\geq 0.11$). In the 54 patients with myocardial creep, 45 (83%) had a change $>10\%$ in MBF and 45 (83%) had a change $>10\%$ in MFR in one of the territories or the whole myocardium.

Table 2: Uncorrected and corrected rest and stress MBF (mL/min/g) and MFR for the three vascular territories (LAD, LCX and RCA) and the whole myocardium (Global).

Vessel		Rest MBF		Stress MBF		MFR	
LAD	Uncorrected	1.2 ± 0.4	(0.5 to 2.7)	2.5 ± 0.9	(0.7 to 5.8)	2.2 ± 0.5	(1.2 to 3.4)
	Corrected	1.2 ± 0.4	(0.5 to 2.7)	2.6 ± 0.9*	(0.8 to 5.6)	2.3 ± 0.6**	(1.4 to 3.8)
LCX	Uncorrected	1.1 ± 0.4	(0.6 to 2.6)	2.5 ± 0.9	(0.8 to 4.8)	2.3 ± 0.7	(0.7 to 5.1)
	Corrected	1.1 ± 0.4	(0.6 to 2.6)	2.5 ± 0.8	(0.7 to 5.4)	2.3 ± 0.6	(0.7 to 3.7)
RCA	Uncorrected	1.2 ± 0.5	(0.6 to 2.7)	4.0 ± 2.3	(1.0 to 9.0)	3.5 ± 1.9	(0.8 to 11)
	Corrected	1.2 ± 0.4	(0.6 to 2.7)	2.7 ± 1.1***	(0.8 to 7.4)	2.4 ± 0.8***	(0.9 to 5.2)
Global	Uncorrected	1.2 ± 0.4	(0.6 to 2.7)	2.7 ± 1.0	(1.0 to 5.7)	2.4 ± 0.7	(1.1 to 5.6)
	Corrected	1.1 ± 0.4	(0.6 to 2.7)	2.6 ± 0.9*	(0.9 to 5.7)	2.3 ± 0.6*	(1.1 to 4.1)

Data are presented as mean ± SD. LAD, left anterior descending; LCX, left circumflex; MBF, myocardial blood flow; MFR, myocardial flow reserve; and RCA, right coronary artery.

* $p<0.05$ ** $p<0.01$ *** $p<0.001$

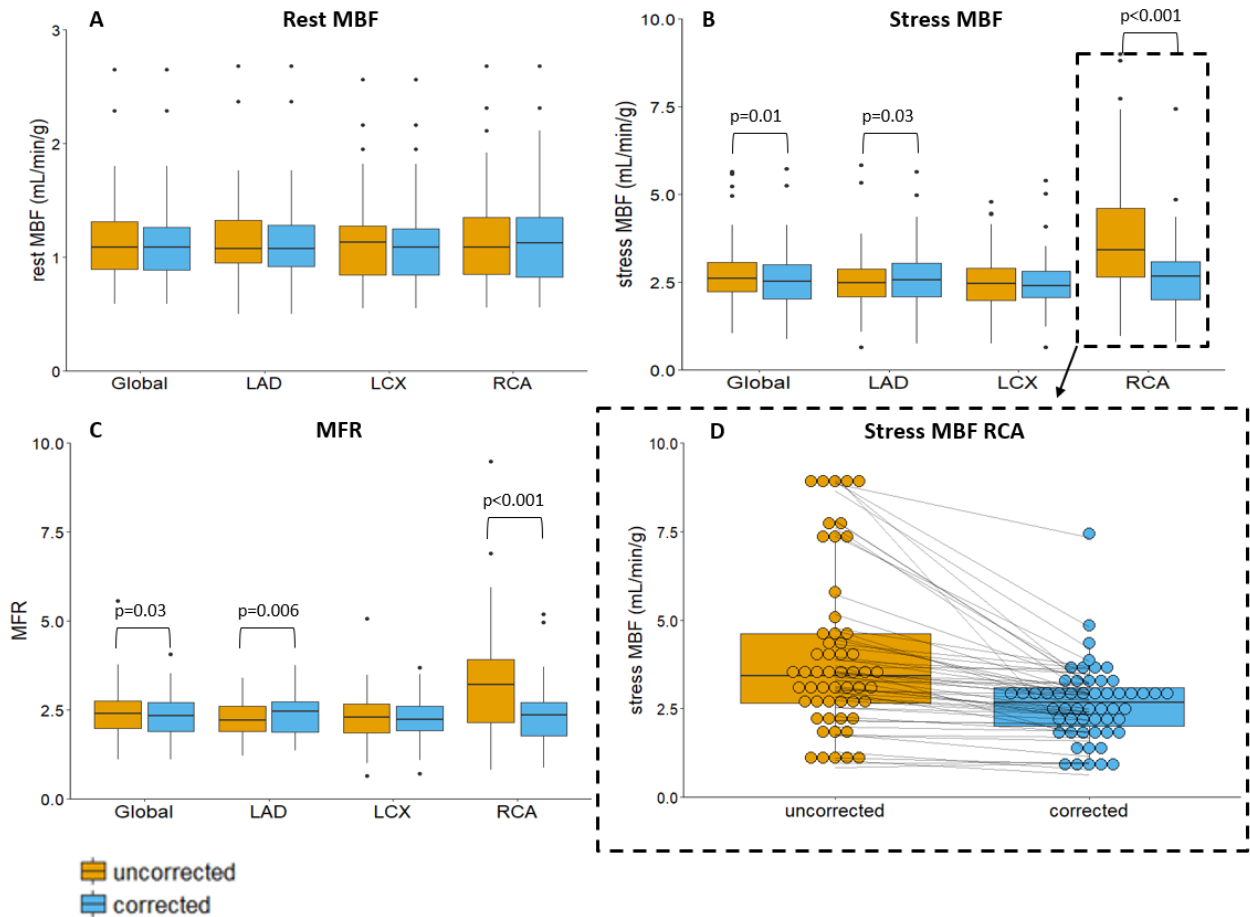


Figure 3: Boxplots showing (A) the rest and (B) stress myocardial blood flows (MBFs) and (C) myocardial flow reserves (MFRs) for the three vascular territories and for the whole myocardium (Global) for the 54 uncorrected and myocardial creep corrected-scans. (D) The stress MBF of the RCA with each point representing one patient scan before and after correction showing MBF decreases in 91% (49/54) of the patients after correction.

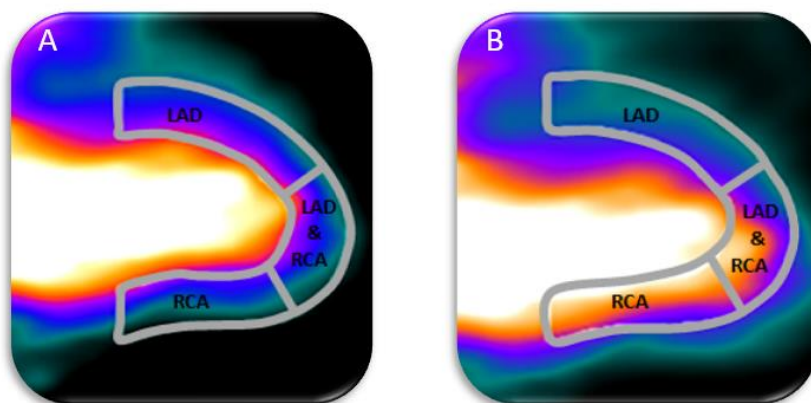


Figure 4: Proper alignment of the automatically drawn myocardium contour and the activity in the heart is shown in A. In case of myocardial creep, there is a misalignment of the drawn myocardium contour with the activity in the heart, as shown in B. This results in increased measured activity in the RCA and partly in the LAD territory.

Discussion

In this study, we have demonstrated that a myocardial creep occurs in more than half of the patients during regadenoson induced stress MPI using Rb-82 PET. Moreover, correction of this myocardial creep resulted in significantly lower MBF and MFR values for the RCA territory and may improve diagnostic accuracy. Besides the large impact on MBF and MFR values in the RCA territory, myocardial creep also resulted in significant differences in stress MBF and MFR for the LAD and the whole myocardium. These differences can be explained by the anatomical position and direction of myocardial creep, as illustrated in Figure 4. During the first-pass phase when the Rb-82 activity is in the LV, there is a strong overlap between the activity and the part of the myocardium contour that is perfused by the RCA and to a lesser extent by the LAD when myocardial creep is present. After correction, the overlap diminishes, which directly affects the MBF and MFR measurements.

Multiple studies have reported the occurrence of myocardial creep, also known as non-returning motion of the heart, primarily occurring in the post-stress period during MPI using different pharmacological vasodilators [47, 50–53]. A recent study by Memmot et al. reported a non-returning motion or myocardial creep in 36% (11/30) of their patients during MPI using Rb-82 PET and regadenoson as vasodilator independent of age [47]. This percentage is in fair agreement with the 52% found in this study although we used a different methodology to assess the presence of myocardial creep and a slightly different time-framing combination. Furthermore, they showed that 69% (11/16) of the patients stressed with regadenoson with visible motion, were categorized as myocardial creep which is in fair agreement to the 78% (54/69) found in our study. Moreover, they reported that only 10% (3/30) of their patients showed significant motion, which was defined as motion greater than half the width of the myocardial wall. Although we did not assess severity or amount of myocardial creep, we did observe that correcting for myocardial creep majorly affected the MBF-quantification in most patients and presumably also in patients with only a limited amount of myocardial creep. Lee et al. recently reported that greater motion was observed during stress, especially in the inferior direction which reflects myocardial creep which is in high agreement with our study [53]. They also reported that motion resulted in the largest MBF and MFR changes in the RCA territory, consisted with our results.

Multiple mechanisms are hypothesized in literature to explain the occurrence of myocardial creep. Karacalioglu et al. hypothesized that myocardial creep is caused by gravity on the organs when patients go from a standing to a lying position in the scanner. They reported that a five minute bed rest on the scanner table significantly decreased the vertical motion of the heart [54]. A CT-scan followed by the rest scan were performed before the stress scan in our protocol. Therefore, the mechanism described above does not explain the myocardial creep we found during stress imaging. Although this gravity theory might explain myocardial creep during rest acquisitions, we observed myocardial creep in only 2% of the rest scans and therefore think this is most likely caused by anxiety at the start of a MPI scan [55].

Another mechanism previously described by Friedman et al. which is more likely to cause myocardial creep is that after administration of a pharmacological vasodilator, in our case regadenoson, lung volume increases which causes a repositioning of the diaphragm and heart [51]. Hence, we are unable to prevent this repositioning of the heart and thus the occurrence of myocardial creep.

Several limitations of this study should be recognized. First we were unable to determine the effect of myocardial creep correction on the diagnostic accuracy due to the lack of a reference standard. However, in some patients myocardial creep resulted in unrealistic high MBF values (>5 mL/min/g) which decreased after correction to realistic values. Hence, we assume that correcting for myocardial creep increases diagnostic reliability.

Secondly, manual actions are required in the quantification process and for the myocardial creep correction which could have introduced additional operator-variability. Although this operator-variability might have introduced additional variance, the changes in stress MBF quantification were higher than the previously reported $\pm 10\%$ test re-test reproducibility errors when calculating the MBF using Rb-82 PET in MPI [56]. Thus, the operator variability is expected to be of limited influence.

Thirdly, a high fraction of the patients had a normal MBF, possibly limiting generalization. However, in case of poorly perfused tissue with myocardial creep, the influence of spillover from the LV is expected to be larger than for normal perfused tissue resulting in a relatively larger overestimation of the modeling parameter k_1 and, hence, MBF [53]. This could result in larger differences between MBF values in the RCA territory before and after myocardial creep correction than reported in this study.

Finally, we only corrected the myocardial creep in the attenuation corrected PET images. However, only the PET data acquired between 2:30 to 7:00 minutes were co-registered to the CT to create an attenuation map. As myocardial creep only occurs in the earlier time frames, misregistration and, hence, attenuation correction artefacts may occur. This misregistration could result in altered MBF measurements [57–60]. Adding a second low-dose CT-scan immediately before the stress PET acquisition is unlikely to improve PET/CT registration as the myocardial creep misregistration occurs after induction of stress and is only temporarily. However, we believe that frame-based co-registration of the stress-PET and CT data can improve PET/CT registration and thereby the reliability of Rb-82 PET quantification in patients with myocardial creep [53].

New knowledge gained

If myocardial creep is present but remains uncorrected in clinical practice, the stress MBF and MFR of the RCA territory will be overestimated, as shown in Figure 3D, which can lead to incorrect diagnosis. The MFR of the RCA may fall within the normal range of the MFR values (>1.7) while after correcting for myocardial creep the MFR drops below this threshold, affecting the diagnosis [40]. Moreover, Memmot et al. showed that myocardial creep occurs more frequently when adenosine is used as pharmacological vasodilator (96%) in comparison to regadenoson (69%) [47]. Therefore, we strongly recommend to check the presence of myocardial creep in all patients regardless of the used pharmacological vasodilator and correct for it to achieve reliable MBF and MFR measurements.

There are two practical ways to recognize myocardial creep in clinical practice. The first sign is an elevated time activity concentration of the RCA during the first pass phase in the TAC in comparison to the LCX and LAD. As no activity is yet present in the myocardium, all activity measured in this phase is due to spillover and should therefore be constant across the three vascular territories, as shown in Figure 1. The second sign is misalignment between the automatically drawn myocardium contour and the observed activity during the first pass phase. As in 83% of our patients with

myocardial creep an MBF change >10% occurred after correction, this implies that even a small myocardial creep should be corrected in clinical practice.

Conclusions

Myocardial creep was seen in 52% of the patients who underwent regadenoson induced stress Rb-82 PET. Correcting for myocardial creep significantly changed MBF measurements during stress and MFR quantification, especially in the RCA territory. As this may hamper diagnostic accuracy, detection and correction of myocardial creep seems necessary for reliable quantification when using regadenoson.

Chapter 3

How to detect and correct myocardial creep in myocardial perfusion imaging using Rubidium-82 PET?

J. Nucl. Cardiol. 2018

(in press)

Authors

S.S. Koenders, BSc^{1,4}, J.D. van Dijk, MSc, PhD¹, P.L. Jager, MD, PhD¹, J.P. Ottervanger, MD, PhD³, C.H. Slump, PhD⁴, J.A. van Dalen, PhD²

Isala hospital, Department of ¹Nuclear Medicine, ²Medical Physics, ³Cardiology, Zwolle, the Netherlands and ⁴MIRA: Institute for Biomedical Technology and Technical Medicine, University of Twente, Enschede, the Netherlands

Abstract

Reliability of myocardial blood flow (MBF) quantification in myocardial perfusion imaging (MPI) using PET can majorly be affected by the occurrence of myocardial creep when using pharmacologically-induced stress. In this paper we provide instructions on how to detect and correct for myocardial creep. For example, in each time frame of the PET images the myocardium contour and the observed activity have to be compared to check for misalignments. In addition, we provide an overview of the functionality of commonly used software packages to perform this quality control step as not all software packages currently provide this functionality. Furthermore, important clinical considerations to obtain accurate MBF measurements are given.

Introduction

Myocardial blood flow (MBF) quantification in myocardial perfusion imaging (MPI) using Rubidium-82 (Rb-82) PET provides valuable information about the extent and functional importance of possible stenosis [3–5]. However, the reliability of MBF quantification can be affected by the occurrence of myocardial creep, in particular during stress imaging [61]. This myocardial creep is presumably caused by the increasing respiration and lung volume and thereby repositioning of the diaphragm and heart after administration of a pharmacological vasodilator [47, 51]. It mainly affects activity concentration measurements in the right coronary artery (RCA) territory as illustrated in Figure 1 [61]. As activity concentration measurements are used in compartmental analyses to derive MBFs, it is essential that these measurements are reliable to prevent biased MBF measurements and thereby false diagnostic interpretation [61].

In our recent study we observed a myocardial creep during regadenoson-induced stress in 52% of the 104 consecutively included patients [61]. In 83% of these 54 patients myocardial creep resulted in a MBF change >10%, which may influence diagnostic interpretation. Although our study only comprised regadenoson-induced stress, the presence of myocardial creep is also reported with adenosine as pharmacological vasodilator [47]. In a limited amount of patients (2%) myocardial creep can also affect MBF quantification using rest imaging [61]. As MBF quantification can become biased when myocardial creep remains uncorrected, detection and correction are necessary for all pharmacological vasodilators and for both rest and stress scans. In this paper we show how myocardial creep can be detected and corrected. Furthermore, we provide an overview of the possibilities of commercially available software packages to detect and correct myocardial creep and highlight important clinical considerations.

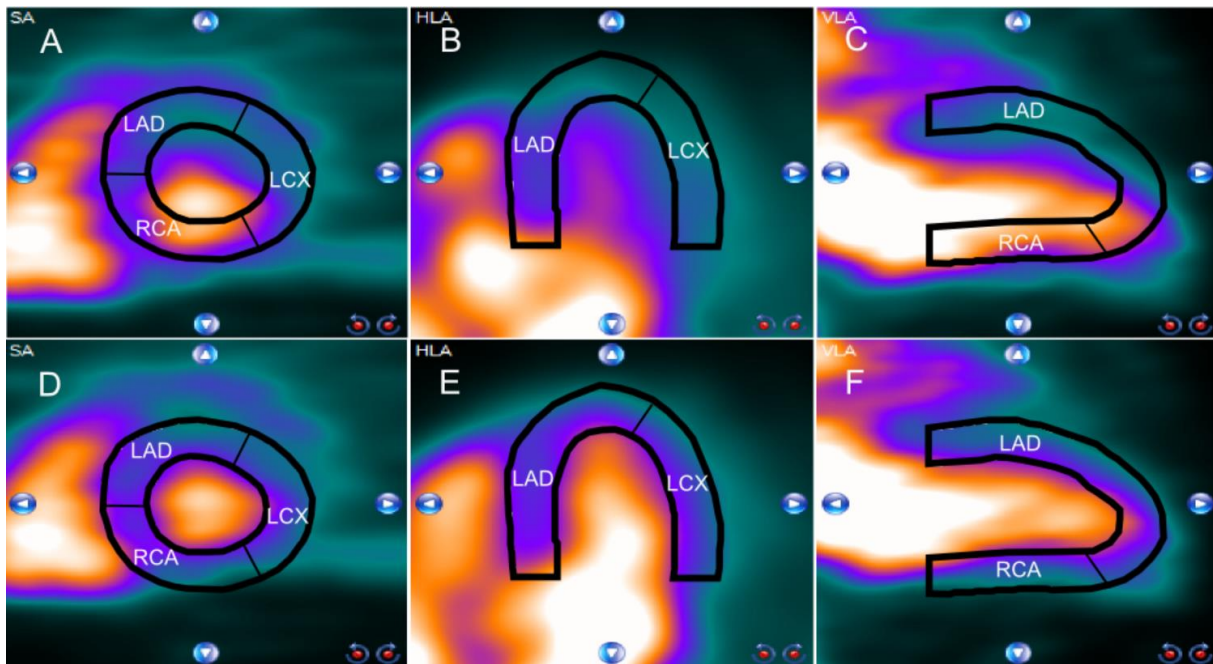


Figure 1: Example of a stress Rb-82 PET scan of a patient with myocardial creep, before (A-C) and after myocardial creep correction (D-F). The myocardium contour is shown in black and the vascular trajectories that primarily supply certain areas of the myocardium with blood are indicated. The appearance of myocardial creep is indicated by the misalignment between the observed Rb-82 activity and the myocardium contour (A-C). Especially the activity concentration in the right coronary artery (RCA) territory is affected when comparing the uncorrected (A-C) with the corrected images (D-F). From left to right: the short axis, horizontal axis and vertical long axis. LAD, left anterior descending; LCX, left circumflex artery.

Methodology

Background – MBF quantification

Several steps have to be performed prior to quantification of MBF: 1) dynamic PET acquisition; 2) image reconstruction of the PET data; 3) segmentation of the myocardium contour; 4) derivation of time-activity curves (TACs) of the myocardium and the left ventricle (LV); 5) quality control; and 6) compartmental analyses [36].

The first step starts with a PET acquisition of typically 7 min for both the rest and stress scans directly after Rb-82 administration. Typically, a low-dose CT scan is added to provide an attenuation map of the chest to allow attenuation correction. Next, the PET images are reconstructed in several time frames (step 2) where the first pass phase is generally sampled with small frame durations of five to ten seconds to assure sufficient temporal resolution and prevent under-sampling of the LV TAC [33–35].

Subsequently, a myocardium contour is drawn, based on all data acquired during the tissue phase where a steady state is reached, i.e. data acquired >2:15 minutes after Rb-82 administration (step 3) [32], as the activity is then primarily present in the myocardium. This contour is used to derive the activity concentrations over time for the whole myocardium or a specific myocardial region. The most common regions are those supplied by blood by one of the three main coronary arteries: left anterior descending (LAD), left circumflex (LCX) and RCA. In addition, the activity concentration in the LV is estimated by using, for example, a region of interest (ROI) positioned in the

cavity of the LV. Both the myocardium contour and the LV ROI are used to automatically derive TACs (step 4). To calculate the MBF for the whole myocardium or a specific region, the TACs from the corresponding myocardial area and the LV are used as input for compartmental analyses. The one-tissue compartment model is most commonly used for this analysis when using Rb-82 (step 6) [8].

To obtain reliable MBF measurements, a quality control (step 5) has to be performed which covers the detection and correction of myocardial creep. We previously defined myocardial creep as a gradual decreasing misalignment of the myocardium contour with the activity present in the ventricle and/or myocardium primarily in the inferior direction [61]. Myocardial creep should be corrected if the misalignment is more than one third of the width of the left ventricular myocardial wall and is present in at least 2 time frames in the first pass phase [61].

Myocardial creep detection and correction

As it is essential to check and correct for myocardial creep [61], we first provide instructions for detection and correction in general, followed by an example based on commercial processing software (Corridor4DM, Invia).

General procedure

The detection and correction procedure consists of seven steps, as shown in Figure 2 A-G. After the PET data are acquired (A), the geometric position of the myocardium contour has to be determined (B) to detect myocardial creep. This is generally done by reconstructing the PET data collected after 2:15 minutes into one image, as the activity is then primarily present in the myocardium. It is important that this image reconstruction is based on a sufficient number of photon counts to provide a clear image of the myocardium. Next, the geometric position of the myocardium can be obtained by drawing a 3D ROI with a fixed threshold of typically 70% of the maximum pixel value in the myocardium (C). The myocardium contour then needs to be copied to all the other time frames of the dynamic acquisition. After the TACs are calculated (D) the position of the 3D ROI and the observed activity distribution in each frame have to be compared (E) as misalignment may indicate myocardial creep.

If myocardial creep is present, it can be corrected for by estimating the misalignment in the x-, y- and z-direction for each time frame in which myocardial creep is visible (F). This geometrical translation can be used to realign the observed activity to the myocardium contour by for example changing the initial coordinates in the DICOM header of the PET data for each of the time frames containing myocardial creep. The calculation of the TACs then has to be repeated to calculate reliable MBFs (G).

Detection and correction procedure for myocardial creep

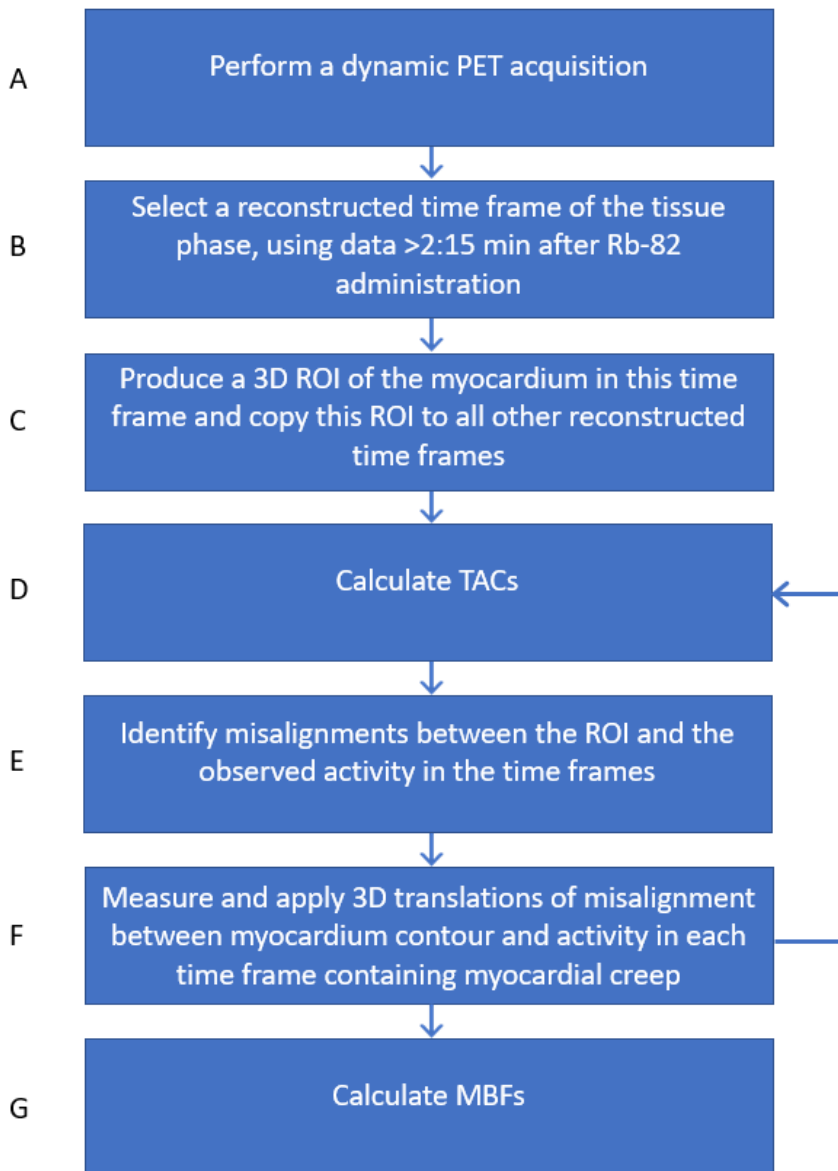


Figure 2: General procedure for the detection and correction of myocardial creep.

Illustration using commercial software

It is possible to perform the detection and correction steps in some commercially available software, for example in Corridor4DM v2016. This software automatically derives an image reconstruction of the acquired PET data between 2:30 and 6:00 min after Rb-82 administration. After assigning the three cardiac axes, a myocardium contour is automatically drawn in the PET image which can manually be optimized if needed. Next, the user has to manually position a ROI at the center of the mitral valve. This ROI is used to estimate the activity concentration in the LV, as illustrated in Figure 3 A. The myocardium contour is then automatically projected to all time frames of the dynamic PET series. Corridor4DM has the option to scroll through the time frames which makes it possible to detect myocardial creep, as shown in Figure 3 B. Myocardial creep can also be identified by observing the TACs. The TAC of the RCA territory then typically shows a higher peak during the first pass phase

compared to those of the other territories (Figure 3 C). This higher peak is due to motion of the heart in the inferior direction, which is related to myocardial creep.

Besides detecting myocardial creep, Corridor4DM also provides the possibility to correct for this movement by manually realigning the myocardium contour with the activity for each individual time frame, as shown in Figure 3 D. After applying this manual realignment in each time frame with myocardial creep, the peaks of the TACs of the three vascular territories (LAD, LCX and RCA) become comparable (Figure 3 E). This ensures the user that a reliable correction for myocardial creep is performed, allowing reliable MBF measurements.

Availability in commercial software packages

As myocardial creep may hamper diagnostic interpretation, accurate detection and correction of myocardial creep are necessary for reliable MBF quantification. Although the detection is most of the time straightforward, correction can be complicated and is not always feasible in the clinical routine due to missing functionality of the used software. From the latest versions of four commonly known and used commercially software packages to quantify MBF using Rb-82 PET, Corridor4DM and QPET (Cedars-Sinai) have the ability to visually evaluate the detection and correction of myocardial creep. SyngoMBF (Siemens Healthcare) provides the functionality to automatically detect and correct for motion, such as myocardial creep, but does not provide insight in the accuracy of the correction. Moreover, it is not possible to manually adjust this correction. Lastly, FlowQuant (University of Ottawa Heart Institute) currently does not have a feature for detection and correction of myocardial creep.

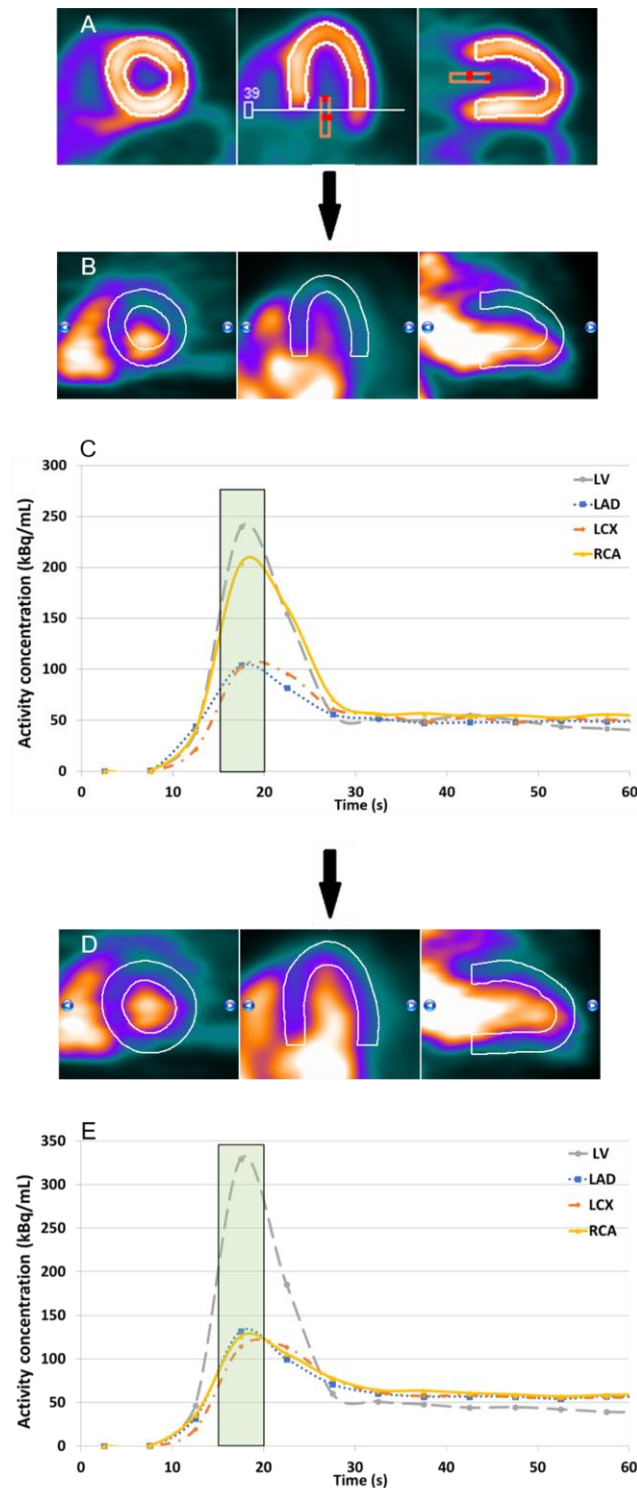


Figure 3: Overview of the three main steps to detect and correct for myocardial creep using Corridor4DM. The myocardium contour is drawn by assigning the most basal part of the septum which still contains activity and the activity concentration in the left ventricle (LV) is measured by placing a region of interest (ROI) manually at the center of the mitral valve (A). To detect myocardial creep, the observed activity in the myocardium has to be compared visually with the myocardium contour in each time frame. The misalignment in the time frame from 15 to 20 seconds shown in (B) indicates myocardial creep. The first 60 seconds of the TAC of this timeframe (C) shows a higher peak in the right coronary artery (RCA) territory compared to those of the other two vascular territories, indicating myocardial creep. In (D), the observed activity in the myocardium is realigned to the myocardium contour. This results in comparable peaks of the TACs of the three vascular territories (E). From left to right (A, B & D): the short axis, horizontal axis and vertical long axis. LAD, left anterior descending; LCX, left circumflex artery.

Considerations

Measurements of MBF using Rb-82 PET are affected by many methodological factors such as differences in equipment, acquisition and reconstruction settings, processing software, tracer infusion, temporal sampling and compartmental analyses [8]. Awareness of all potential pitfalls and underlying assumptions in methodology are essential for using MBF measurements in clinical practice. For example, it is important that a constant activity injection profile is used together with an adequate number and length of time frames, to prevent under sampling and that myocardial creep is adequately corrected.

Although we focused on Rb-82 PET, it is likely that myocardial creep occurs in a similar way using other PET tracers such as Oxygen-15 water and Nitrogen-13 ammonia. Therefore, detection and correction should always be performed in quantitative PET MPI studies, independent of the tracer. Physicians should always check for accurate myocardial creep correction before clinical interpretation. This can be performed by inspecting the TAC for an elevated peak of the RCA during the first pass phase in comparison to the LAD and LCX as shown in Figure 3 C [61]. Physicians can also visually assess the individual time frames for misalignments between the myocardium contour and the activity in the myocardium as shown in Figure 3 B.

In conclusion, adequate detection and correction of myocardial creep are crucial for reliable MBF quantification. To adequately perform the required quality control, it is not only important that software packages provide the possibility to detect and correct myocardial creep, but also that users can visually inspect and evaluate these steps. Hence, vendors should provide this functionality or adapt their software accordingly.

Chapter 4

**Simulation of myocardial blood flow
quantification using a
one-tissue compartment model
provided in R**

Abstract

Background: TracerRkinetic is a script provided in R that makes it possible to implement the one-tissue compartment model of Lortie et al. in the programming language of R which can be used to calculate myocardial blood flow (MBF). The effect of several factors on MBF measurements can be simulated using this script which would provide a time saving and patient friendly solution. Our aim was to assess if the quantification of MBF using the implemented one-tissue compartment model provided in R results in comparable MBF measurements as when Corridor4DM software is used.

Methods: We analysed 19 cardiac studies in both rest and stress conditions. Rest and stress MBF and MFR (stress MBF/rest MBF) were calculated. Results obtained with the one-tissue compartment model provided in RStudio were tested against the Corridor4DM package.

Results: There is an excellent agreement for the rest MBF, stress MBF and MFR ($r > 0.99$, $p < 0.001$). Systemic biases of -0.05 mL/min/g ($p < 0.001$) and -0.10 mL/min/g ($p < 0.001$) were found for the rest and stress MBF.

Conclusion: Quantification of MBF using the one-tissue compartment model provided in the programming language of R is comparable to Corridor4DM. Therefore, the R script provides a time saving tool for simulation of MBF quantification in Rb-82 PET.

Introduction

In the process of myocardial blood flow (MBF) quantification using Rubidium-82 (Rb-82) PET, there are several factors which can be optimized. As performing studies on these factors on a PET system are time-consuming and require prospective patient studies, simulation of these factors and their effect on MBF quantification would provide a time saving and patient friendly solution. Mateos-Pérez et al. provided a script called TracerRkinetic that makes it possible to implement the one-tissue compartment model of Lortie et al. in the programming language of R [7, 62]. The relevant equations to solve the compartment model and which are implemented in R for Rb-82 cardiac studies are:

$$C_m(t) = K_1 e^{-k_2 t} \otimes C_a(t) \quad (1)$$

With $C_m(t)$ the activity concentration in the myocardium (tissue), $C_a(t)$ the activity in the left ventricle (LV) and K_1 and k_2 are rate constants [7, 62]. The second equation needs to be solved because there has to be corrected for spillover:

$$C_{PET}(t) = v_B C_a(t) + (1 - v_B) C_m(t) \quad (2)$$

with $C_{PET}(t)$ the time activity curve (TAC) obtained with the manual placed region of interest (ROI) in the dynamic PET data and v_B the fraction of blood in the tissue. K_1 can be obtained using the Renkin-Crone equation:

$$K_1 = \left(1 - a e^{-\frac{b}{MBF}}\right) MBF \quad (3)$$

Where $a=0.77$ and $b=0.63$ mL/min/g to correct for the non-linear Rb-82 extraction as a function of MBF. The weights for the fitting process are proportional to frame length. The input functions for R are the activity concentrations over time present in the LV and in the tissue regions: left anterior descending (LAD), left circumflex (LCX), right coronary artery (RCA) and for the whole myocardium (global) together with the frame times. Mateos-Pérez et al. showed that the implemented compartment model in R had comparable results as PMOD and can be used to solve studies where the activity concentrations in regions of interest (ROIs) are already determined [62]. Our aim was to assess if the quantification of MBF using the implemented one-tissue compartment model provided in R provides comparable results as Corridor4DM.

Method

Patient preparation and data acquisition

All subjects were asked to abstain from caffeine-containing substances for 24 hours and to discontinue dipyridamole containing medication for 48 hours before imaging. Prior to myocardial perfusion imaging, a low-dose CT scan was acquired during free-breathing to provide an attenuation map of the chest. This scan was made using a 5 mm slice thickness, 0.8 s rotation time, pitch of 0.97, collimation of 32x0.625 mm, tube voltage of 120 kV and tube current of 10 mA. Next, 740 MBq Rb-82 was administered intravenously with a flow rate of 50 mL/min using a Sr-82/Rb-82 generator (CardioGen-82, Bracco Diagnostics Inc.). After the first elution, we induced pharmacological stress by administrating 400 µg (5 mL) of regadenoson over 10 seconds. After a 5 mL saline flush (NaCl 0.9%)

we administered a second dose of 740 MBq Rb-82. We acquired seven minute PET list-mode acquisitions following both Rb-82 administrations. Attenuation correction was applied to all data after semi-automatic alignment of CT and PET data.

Corridor4DM versus RStudio

We analysed 19 PET Rb-82 rest and stress studies. Corridor4DM (v2016) was used to obtain ROIs in both the rest and stress scan. These were used to calculate the TACs. The TACs were modelled in Corridor4DM using the one-tissue compartment model of Lortie et al. to calculate the rest and stress MBF. Furthermore, myocardial flow reserve (MFR) was calculated (stress MBF / rest MBF) [7]. The weighting for calculating both rest and stress MBF and MFR was set at frame length. The individual activity concentrations of the LV, vascular territories (LAD, LCX and RCA) and whole myocardium in the 26 time frames together with the start and end time of the 26 frames were exported from Corridor4DM as text file. Next, the text files were manual adjusted in excel to anonymize the data for further processing in RStudio and to serve as input functions for MBF quantification. Rest and stress MBF and MFR were calculated using RStudio (Version 1.0.143 – © 2009-2016 RStudio, Inc.). Results obtained with the one-tissue compartment model provided in RStudio were tested against the Corridor4DM package.

Statistical analyses

The correlation between Corridor4DM and RStudio for the rest and stress MBF and MFR were assessed using Pearson correlation scores. Bland-Altman plots and paired samples t-tests were used to assess for systemic biases for the rest and stress MBF and MFR using all data of the three vascular territories (LAD, LCX and RCA) and the whole myocardium (global). A p-value of <0.05 was considered as statistical significant.

Results

There was an excellent agreement in the results, either for the rest and stress MBF and MFR for the individual territories and for the whole myocardium as shown in Figure 1 A,C & E ($r>0.99$, $p<0.001$). Systemic biases were found for the rest and stress MBF of -0.05 mL/min/g ($p<0.001$) and -0.10 mL/min/g ($p<0.001$) as shown in Figure 1 B & D.

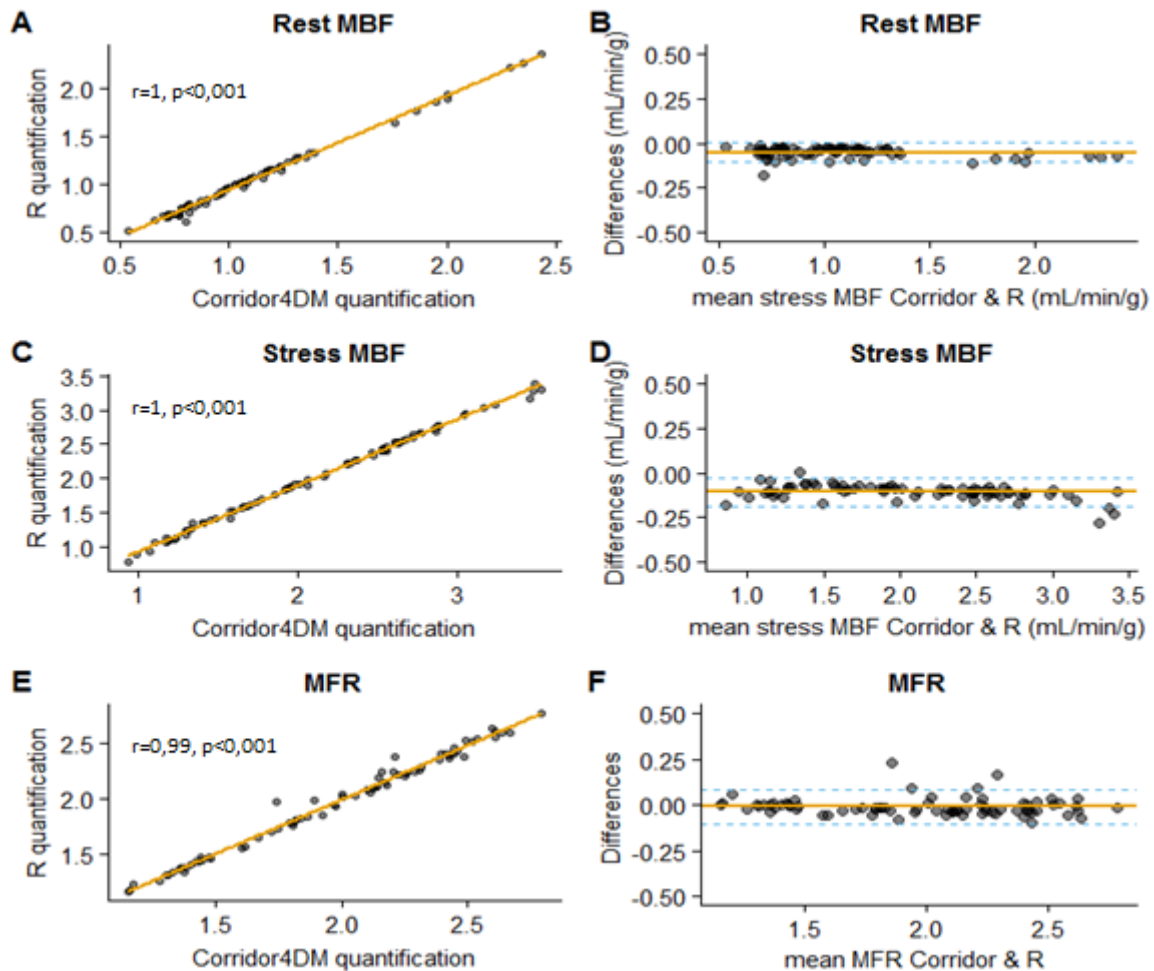


Figure 1: Regression plots showing the comparison between the rest (A) and stress (C) MBF and MFR (E) calculated with RStudio and Corridor4DM. The blue dotted line is the line of identity. The Bland-Altman plots of the rest (B) and stress (D) MBF and MFR (F) showing the mean difference (yellow line) and the 95% CI (blue dotted lines). Systemic biases were found for the rest (B) and stress (D) MBF.

Discussion

In this study we showed that the implementation of the one-tissue compartment model in R can be used to quantify MBF when segmentations of ROIs have been previously performed with Corridor4DM. We have shown excellent correlation. We found a systemic biases for the rest and stress MBF.

Excellent agreement ($R^2 > 0.99$, $p < 0.001$) was also found by Mateos-Pérez et al. [62]. They compared the implemented one-tissue compartment model in R with the PMOD package. They found no evident bias in the results where we found systemic biases in the rest and stress MBF measurements calculated in R compared to MBF and MFR measurements calculated with Corridor4DM.

Although we included more cardiac studies than Mateos-Pérez et al. [62] (19 vs 8), the implementation was still assessed on a limited number to test if the results are comparable to Corridor4DM. Furthermore, there is still interaction required with the Corridor4DM software whereas the R script cannot employ the segmentations that have to be performed for calculating the

activity concentrations in the different time frames. However, once the TACs derived from the segmentations are exported, they can be manually adjusted to predict the effect of several factors on the MBF quantification and to simulate if these are worthwhile for validation.

Although we found a systemic bias and the sample size was small, the high correlation indicate that the provided script in R can be used to simulate MBF and MFR quantification. This enables the assessment of several optimization possibilities within R without wasting time and prevents testing multiple protocols on patients. Therefore, the provided script in R is a time saving and patient friendly method to test hypothesis and can be used to select the most promising results which then can be tested on the PET-scanner for validation.

Conclusions

This study shows that quantification of MBF using the one-tissue compartment model provided in the programming language of R is comparable to MBF quantification in Corridor4DM. Therefore, the R script provides a time saving tool for simulation of MBF quantification in Rb-82 PET.

Chapter 5

Minimization of temporal sampling for myocardial blood flow quantification using Rubidium-82 PET

Abstract

Background: Temporal sampling in dynamic Rubidium-82 (Rb-82) PET studies influences myocardial blood flow (MBF) quantification. Both the length and the number of time frames influence measured time activity curves (TACs) that are used as input for compartmental analysis to obtain MBFs. A large number of time frames imply time-consuming reconstructions which may hamper clinical implementation. Our aim was to determine a temporal sampling protocol with the minimum number of time frames that still result in precise MBF measurements using Rb-82 PET.

Methods: We retrospectively included 30 consecutive patients (15 with an ejection fraction (EF) <45% and 15 with an EF ≥45%) who underwent dynamic rest and pharmacological induced (regadenoson) stress Rb-82 PET/CT (GE Discovery 690, GE Healthcare). Data were reconstructed using 26 time frames (12x5s, 6x10s, 4x20s, 4x40s). Activity concentrations during stress were determined in the left ventricle (LV), the three vascular territories: left anterior descending (LAD), left circumflex (LCX) and right coronary artery (RCA) and in the whole myocardium (global) for each time frame using Corridor4DM software (INVIA, v2016). Next, we simulated the TACs for different temporal sampling protocols varying between 20 and 14 frames. MBFs were quantified with TracerKinetic software using the Lortie one-tissue compartment model. Temporal sampling protocols were considered for validation if the SD of the relative differences was ≤5%. Again 30 consecutive patients (15 with an EF <45% and 15 with an EF ≥45%) were retrospectively included. Two temporal sampling protocols, with 20 and 14 frames, were validated by reconstructing dynamic data sets using these protocols. MBFs were calculated and compared to the currently used protocol with 26 frames. Temporal sampling protocols were considered for clinical adoption if the SD of the relative differences lied within the methodological precision of 10%.

Results: Six protocols were considered for validation: the protocol with 14 (2) frames (9x10s, 3x30s, 1x60s, 1x120) had a SD of the relative differences for the global MBF of 3.7%; 14 (3) frames (9x10s, 3x30s, 1x60s, 1x120s) had a SD of the relative differences of 4.5%; 16 (2) frames (12x10s, 2x30s, 1x60s, 1x120s) of 4.2%; 17 (1) frames (12x5s, 3x20s, 2x120s) of 4.4%; 18 frames (12x5s, 2x10s, 2x20s, 2x120s) of 3.8 % and 20 frames (12x5s, 6x10s, 2x120s) had a SD of the relative differences for the global stress MBF of 3%. The protocol with 20 and 14 (12x10s, 2x120s) frames were validated and had a SD of the relative differences for rest and stress global MBF of 5.1%, 7.0%, 6.1% and 6.6%, respectively.

Conclusion: The choice of temporal sampling protocol influences MBF outcomes. Temporal sampling protocols with less than 26 frames still result in precise MBF quantification using Rb-82 PET. The minimal number of time frames that can be considered for clinical adoption is 14.

Introduction

Temporal sampling in dynamic Rubidium-82 (Rb-82) PET studies influences myocardial blood flow (MBF) quantification. A temporal sampling protocol is used in cardiac PET to reconstruct dynamic images. The activity concentrations in these dynamic images are measured using regions of interest (ROI's) to obtain time activity curves (TAC) which show the radiotracer concentration as a function of time in the tissue represented by the ROI. These TACs are used as input for compartmental analysis to obtain MBFs. Both the length and the number of time frames of the used temporal sampling protocol influence measured TACs. Shorter time frames will result in an increase in temporal resolution but it will also increase noise [34]. Furthermore, a large number of time frames imply time-consuming reconstructions which may hamper clinical implementation.

The calculated TAC can be divided into a first pass phase where activity reaches the left ventricle (LV) and a tissue phase in which activity is distributed to the myocardium. These periods have to be sampled accurately to obtain accurate MBF measurements [34]. The first pass phase is generally sampled with small frame durations of five to ten seconds [33–35]. Lee et al. have shown that a simple two-phase framing, with the first pass phase having 24 frames with durations of 5 seconds and the tissue phase having frame durations up till 120 seconds, optimally samples the LV TAC for modern 3D PET systems [34]. This results in a total number of 26 time frames (24x5s, 2x120s). Although Lee et al. showed that the optimal temporal sampling protocol consists of 26 time frames, they did not assess the minimal number of time frames. Less time frames will decrease reconstruction time and might provide the possibility for a “one-stop shop”. Therefore, our aim was to determine the minimal number of time frames for Rb-82 PET MPI that still results in precise MBF measurements compared to currently used protocol with 26 time frames at the nuclear department of Isala.

Method

Study population

We evaluated dynamic Rb-82 rest and stress data from 60 retrospectively included patients referred for MPI using Rb-82 PET (GE Discovery 690, GE Healthcare) who underwent dynamic rest and regadenoson induced stress. Of these 60 patients 30 were used for the first part of the study and 30 for the second part of the study. Of the 30 patients in both groups, 15 patients fulfilling the criteria of an ejection fraction (EF) larger than or equal to 45% and 15 with an EF of less than 45% were included in a consecutive manner. All patients provided written informed consent for the use of data for research purposes. As all analyses were carried out retrospectively, no approval from the ethical committee was required according to Dutch law.

PET imaging

All subjects were instructed to abstain from caffeine-containing substances for 24 hours and to discontinue dipyridamole containing medication for 48 hours before imaging. Prior to MPI, a low-dose CT scan was acquired during free-breathing to provide an attenuation map of the chest. This scan was made using a 5 mm slice thickness, 0.8 s rotation time, pitch of 0.97, collimation of 32x0.625 mm, tube voltage of 120 kV and tube current of 10 mA. Next, 740 MBq Rb-82 was administered intravenously with a flow rate of 50 mL/min using a Sr-82/Rb-82 generator (CardioGen-

82, Bracco Diagnostics Inc.). After the first elution, we induced pharmacological stress by administering 400 µg (5 mL) of regadenoson over 10 seconds. After a 5 mL saline flush (NaCl 0.9%) we administered a second dose of 740 MBq Rb-82. We acquired seven minute PET list-mode acquisitions following both Rb-82 administrations. Attenuation correction was applied to all data after semi-automatic alignment of CT and PET data.

Image processing

The dynamic data sets were reconstructed using 26 time frames (12x5s, 6x10s, 4x20s, 4x40s) with the default settings as recommended by the manufacturer using 3D iterative reconstruction, while correcting for decay, attenuation, scatter and random coincidences, and dead time effects. Neither time-of-flight information, nor a post-processing filter or resolution modelling was used. Static images were reconstructed from 2:30 to 7:00 minutes for both rest and stress scans. Myocardium contours in the dynamic series were drawn semi-automatically using the Corridor4DM software (v2016) based on the static images. Next, a region of interest (ROI) was manually placed at the position of the mitral valve to estimate the activity in the first pass phase (blood pool). The ROI sampling methodology described by Lortie et al. automatically extracts the LV blood pool TAC [7]. The myocardial TACs were estimated from the tracer activity for the three vascular territories, left anterior descending (LAD), left circumflex (LCX) and right coronary artery (RCA) and for the whole myocardium. Next, the TACs of the LV, vascular territories and for the whole myocardium were exported as text file and anonymized in Excel for further processing in RStudio (Version 1.0.143 2009-2016 RStudio, Inc.).

Minimizing number of time frames

We simulated several temporal sampling protocols found in literature that use 10-second frame durations for the first pass phase [33, 63]. Furthermore, we tried several other combinations using 5-seconds frame durations for the first pass phase. Due to variability in first pass phase duration, the LV TACs of the included patients were plotted to determine the maximum first pass phase duration. The first pass phase is defined as the filling of the LV and ends after the peak of the LV TAC where the tissue phase starts. This time interval was chosen as first pass phase and was sampled at 5-second frame durations as recommended by Lee et al. [34]. Moreover, the last 240 seconds of the dynamic series were sampled at 120-seconds frame durations. Next, we varied the remaining time into a variable number of frames and frame durations so that the total number of used time frames decreased compared to currently used 26 time frames.

Simulation of new temporal sampling protocols

To assess the minimal number of time frames possible for dynamic Rb-82 PET MPI, SDs of the relative differences (%) in regional (LAD, LCX and RCA) and global (whole myocardium) stress MBF for the varying temporal sampling protocols were computed for clinical data. The simulated stress MBF values of the 26 time frames were used as reference values to calculate the SD of the relative differences in stress MBF for the three vascular territories (LAD, LCX and RCA) and for the whole myocardium (global) using RStudio. A paired samples t-test was used to test for systemic biases using the global stress MBF. The level of statistical significance was set to 0.05. Absolute MBF values of the whole myocardium and three vascular territories were corrected for systemic biases. Temporal sampling protocols were considered for validation if the SD of the relative differences was ≤5%. We

chose a smaller SD of the relative differences than the methodological precision of 10% because the simulation study does not contain observer variability [56].

Validation of accepted temporal sampling protocols

Dynamic data sets were reconstructed using the 26 time frames and with two of the accepted temporal sampling protocols. Rest and stress MBFs were calculated in Corridor4DM for each temporal sampling protocol. A paired samples t-test was used to test for systemic biases using the rest and stress MBF of the whole myocardium (global). The level of statistical significance was set to 0.05. Absolute rest and stress MBF values of the whole myocardium and three vascular territories (LAD, LCX and RCA) were corrected for systemic biases. Rest and stress MBFs of the 26 time frames were used as reference values for calculating the SDs of the relative differences for the three vascular territories and for the whole myocardium. Protocols were considered for clinical adaptation if the SD of the relative differences for the rest and stress MBF lied within the methodological precision of 10% [56].

Results

Study population

Basic characteristics of the study population are given in Table 1. There were no significant differences between the simulation and validation group.

Table 1: Baseline characteristics of all included patients for the simulation (n=30) and validation (n=30) study who underwent clinically indicated Rb-92 PET MPI.

	Simulation (n=30)	Validation (n=30)	p Values (t-test / χ^2)
Age (years)	66 ± 12	66 ± 10	0.86
Male gender (%)	60	80	0.09
Weight (kg)	88 ± 18	90 ± 17	0.79
Length (cm)	175 ± 11	177 ± 9	0.34
BMI (kg/m ²)	29 ± 6	29 ± 5	0.83
Hypertension (%)	67	53	0.29
Dyslipidemia (%)	40	43	0.79
Diabetes (%)	20	27	0.54
Current smoker (%)	23	17	0.52
Family history (%)	47	47	1.00
Normal MPI scan (%)	60	57	0.79
Ischemic defects on MPI (%)	13	23	0.32
Non-reversible defects on MPI (%)	30	30	1.00

Data are presented as mean ± SD or as percentage

Minimizing number of time frames

Maximum first pass phase duration of the 30 included patients for the simulation study was ± 60 seconds as shown in Figure 1. We tested nine temporal sampling protocols. An overview of the different temporal sampling protocols tested is shown in Figure 2.

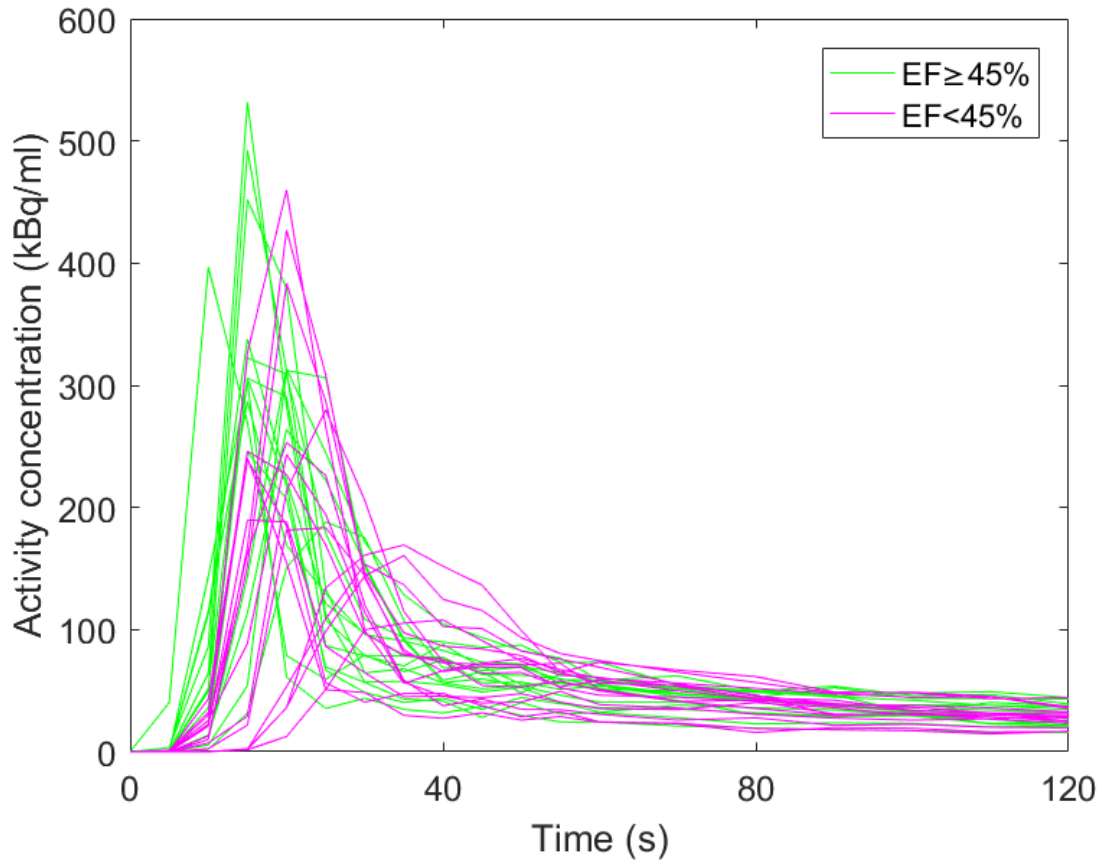


Figure 1: First pass phase of the 30 patients included for the simulation study showing a variety of first pass phase durations with a maximum duration of ± 60 seconds.

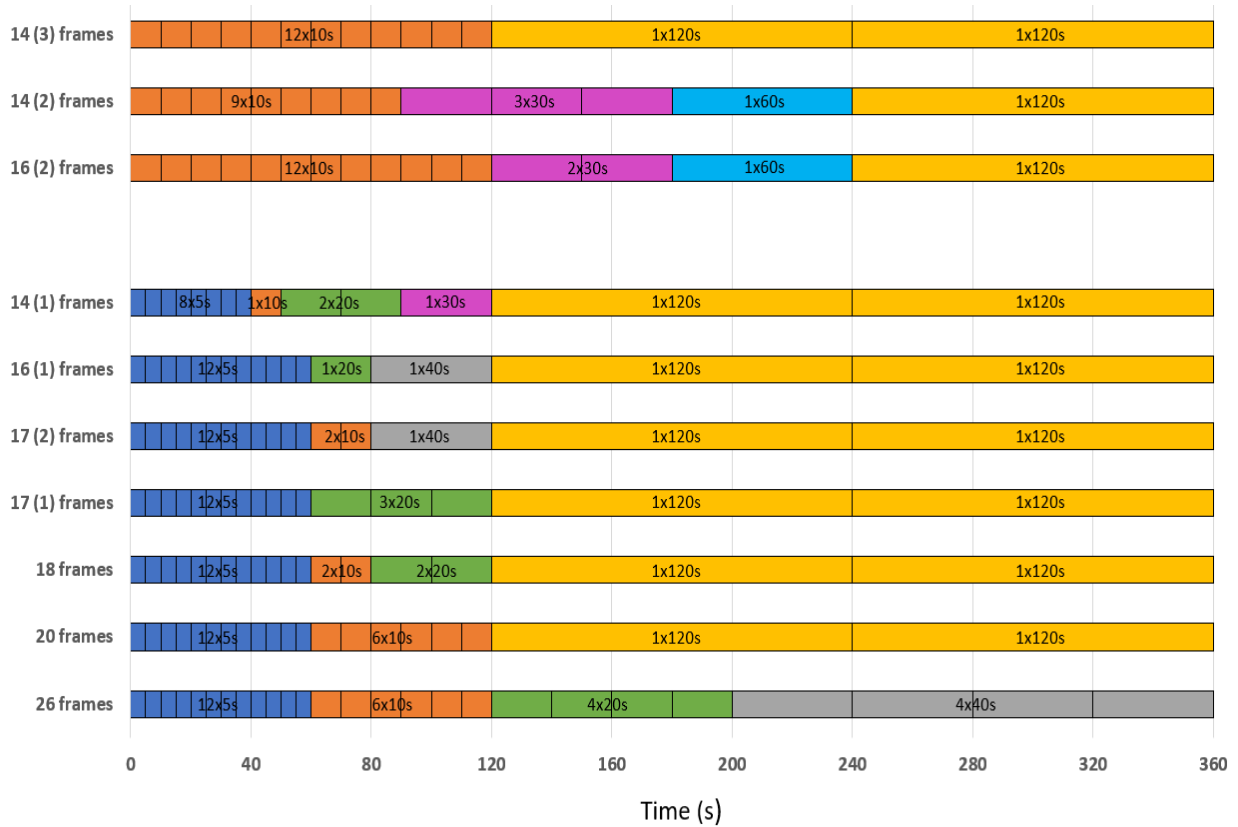


Figure 2: Overview of the nine temporal sampling protocols simulated to evaluate their effect on MBF quantification in comparison to the reference temporal sampling protocol of 26 time frames.

Table 2: Temporal sampling protocols with the SD of the relative differences for the whole myocardium (global) and the three vascular territories (LAD, LCX and RCA) after correction for systemic biases. Absolute biases with the significance are also shown. The level of significance was set to 0.05.

Number of frames	Temporal sampling protocol	SD of the relative differences (%)				Absolute bias	p-values (t-test)
		Global	LAD	LCX	RCA		
20	12 x 5s, 6 x 10s, 2 x 120s	3.0	3.2	3.1	3.1	0.02	0.06
18	12 x 5s, 2 x 10s, 2 x 20s, 2 x 120s	3.8	4.0	4.0	4.0	-0.02	0.047
17 (1)	12 x 5s, 3 x 20s, 2 x 120s	4.4	4.7	4.5	4.8	-0.06	<0.001
17 (2)	12 x 5s, 2 x 10s, 1 x 40s, 2 x 120s	5.7	5.9	5.9	6.4	-0.09	<0.001
16 (1)	12 x 5s, 1 x 20s, 1 x 40s, 2 x 120s	6.5	6.8	6.5	7.7	-0.14	<0.001
14 (1)	8 x 5s, 1 x 10s, 2 x 20s, 1 x 30s, 2 x 120s	7.8	8.1	7.5	9.3	-0.17	<0.001
16 (2)	12 x 10s, 2 x 30s, 1 x 60s, 1 x 120s	4.2	4.6	3.5	5.6	0.09	<0.001
14 (2)	9 x 10s, 3 x 30s, 1 x 60s, 1 x 120s	3.7	4.0	3.1	4.7	0.05	0.001
14 (3)	12 x 10s, 2 x 120 s	4.5	4.9	3.9	5.3	0.09	<0.001

Simulation

Of the nine tested temporal sampling protocols, we found a systemic bias for each tested protocol except for the protocol with 20 frames, as shown in Table 2. Six protocols were considered for validation as shown in Figure 3: the protocol with 14 (2) frames (9x10s, 3x30s, 1x60s, 1x120) had a SD of the relative differences for the global MBF of 3.7%; 14 (3) frames (9x10s, 3x30s, 1x60s, 1x120s) had a SD of the relative differences of 4.5%; 16 (2) frames (12x10s, 2x30s, 1x60s, 1x120s) of 4.2%; 17 (1) frames (12x5s, 3x20s, 2x120s) of 4.4%; 18 frames (12x5s, 2x10s, 2x20s, 2x120s) of 3.8 % and 20 frames (12x5s, 6x10s, 2x120s) had a SD of the relative differences for the global stress MBF of 3%.

Of these six protocols, the ones with 20 and 14 (3) frames were chosen for validation while we wanted to enact that the last 240 seconds can be sampled at 120 seconds and to see the difference between 5 and 10 seconds samples at the beginning of the temporal sampling protocol. Moreover, the 14 frames protocol was the minimal number of time frames accepted during simulation.

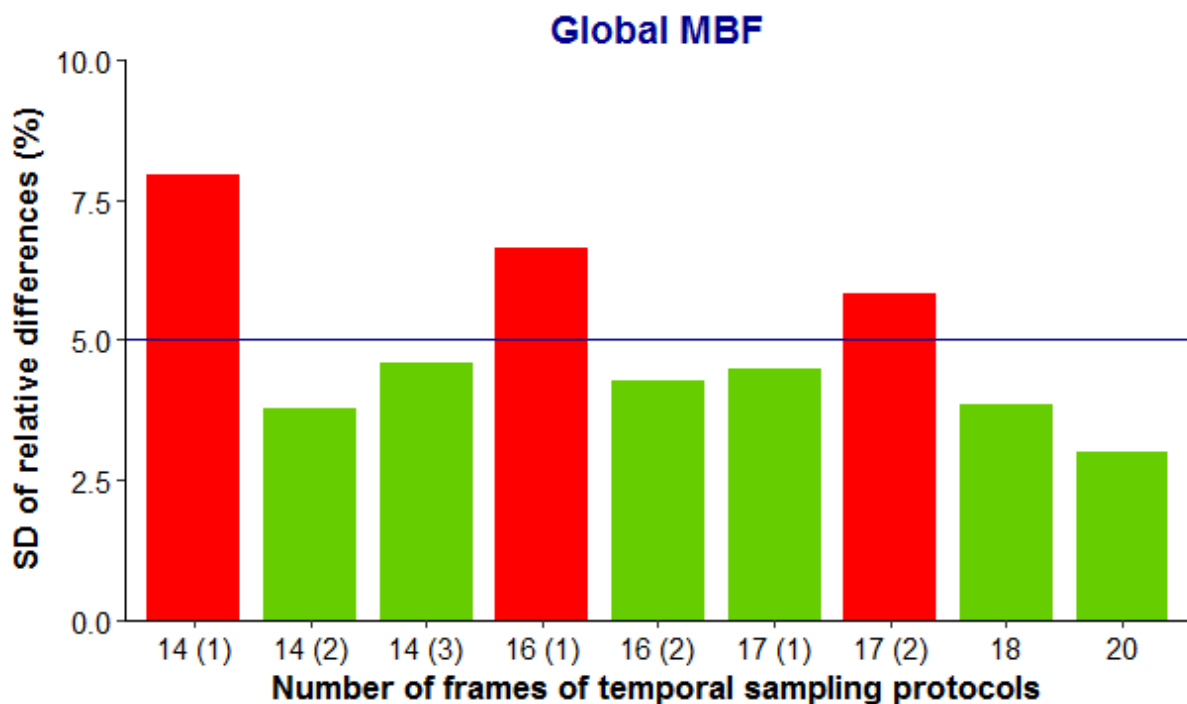


Figure 3: Barplot showing the accepted temporal sampling protocols (green) with a SD of the relative differences $\leq 5\%$ and the temporal sampling protocols that are not accepted (red) with a SD of the relative differences $> 5\%$.

Validation

The SD of the relative differences for rest and stress MBF quantifications in the whole myocardium (global) and for the three vascular territories for the protocols with 20 and 14 frames compared to the protocol 26 frames are listed in Table 3. A systemic bias of 0.11 was found for the protocol with 20 frames. The smallest SD of the relative differences was found for the global MBF which are shown in Figure 4. The SD of the relative differences for global rest and stress MBF using 20 frames compared to 26 frames were 5.1% and 7.0%, respectively. When comparing 14 frames with the 26 frames protocol, the SD of the relative differences for global rest and stress MBF were 6.1% and 6.6%, respectively. The largest SDs of the relative differences with a maximum of 12.1% was found for the RCA territory.

Table 3: SD of the relative differences (%) of rest and stress MBF between the protocol with 26 frames versus 20 and 14 frames for the global perfusion and the three vascular territories: LAD, LCX and RCA. A systemic bias was found for the protocol with 20 frames.

Number of frames	Rest/stress	SD of relative differences (%)				Absolute bias	p-values (t-test)
		Global	LAD	LCX	RCA		
20	Rest	5.1	6.9	8.4	12.1	0.11	<0.001
	Stress	7.0	8.0	7.4	12.0		
14	Rest	6.1	8.4	7.8	12.1	-0.002	0.9
	Stress	6.6	6.7	5.9	10.4		

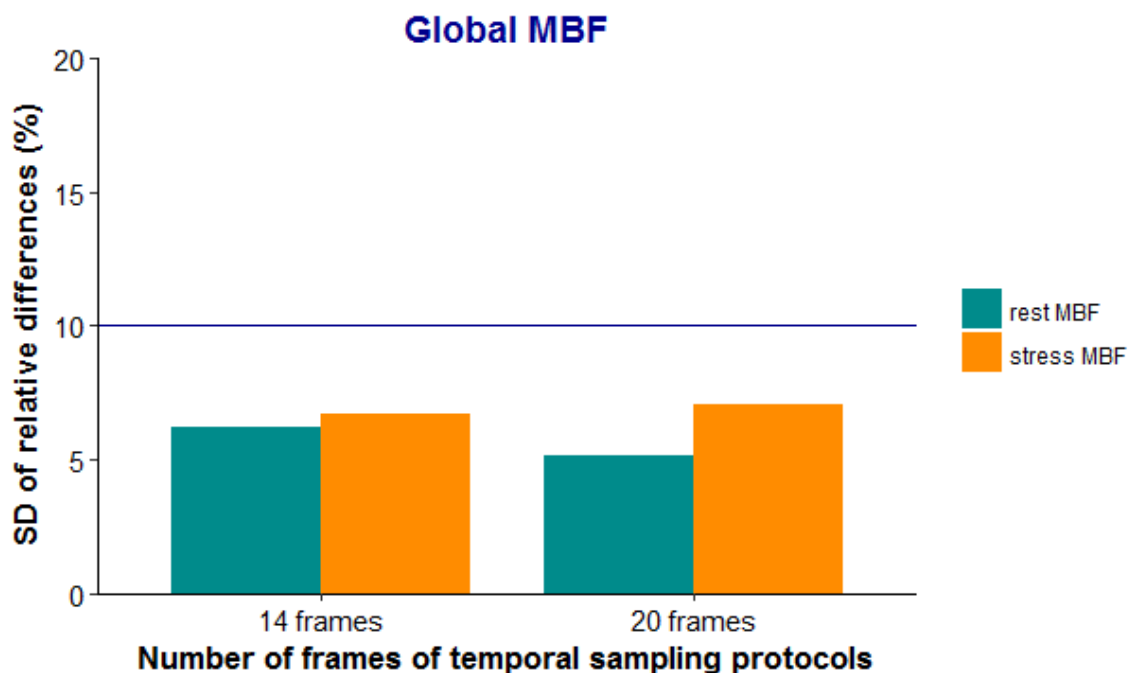


Figure 4: Barplot of the SD of the relative differences (%) for rest and stress global MBF of the temporal sampling protocols with 20 and 14 frames. The temporal sampling protocol with 26 frames was used as reference.

Discussion

In this study we minimized dynamic time frame binning during image reconstruction for Rb-82 PET MPI. The number of frames was minimized to decrease reconstruction time and therefore could provide the possibility for a “one-stop shop”. In the first part of this study we have demonstrated that six of the tested temporal sampling protocols had a SD of the relative differences for global stress MBF $\leq 5\%$. Moreover, validation of two of these protocols, with 20 and 14 frames, showed that MBF measurements had a methodological precision within 10% for global MBF (whole myocardium) and can therefore be considered for clinical adoption.

The results of the temporal sampling protocol with 20 frames of the simulation part of this study show that the last 240 seconds of the dynamic series can be sampled at 120-seconds frame duration with minimal effect on MBF quantification as was shown by Lee et al. [34]. Furthermore, Lee et al showed that the use of a two-phase sampling protocol can be used for optimal sampling which is in agreement with the protocol using 14 frames in this study [34]. However, sampling of the first pass phase with the 14 frame protocol is different. Lee et al. reported that 5 second-frame durations are optimal for the first pass phase but our 14 frame protocol used 10-second frame durations. They recommend a 5-second first pass phase frame duration because the first pass phase duration is not directly controllable by the technologist. We observe variable first pass phase durations in clinical practice. Of the included patients, 50% had an EF of $<45\%$. The first pass phase duration of these patients are in general longer than the ones with an EF of $\geq 45\%$. Furthermore, a pinched vein or increasing generator age might also result in a longer first pass phase duration [10]. The global rest and stress MBF of the 14 frame protocol in the validation part of this study, which used 10-second frame durations for the first pass phase, lied within the methodological precision of 10% reported by Kitkungvan et al. [56]. However, it is imaginable that sharp LV TACs with a short first pass phase duration are better sampled using 5-second frame durations and TACs with a longer first pass phase durations using 10-second frame duration. Raylman et al. even suggest that TACs must be matched to imaging protocols to achieve minimum bias and variance in kinetic parameter estimates [64]. Although this makes sense in theory, this would not be applicable in the clinical routine.

Several limitations of this study should be recognized. The first limitation is the lack of a reference standard in this study. We used the time sampling protocol with 26 frames currently used in the clinical routine as reference standard which is, in our case, the best alternative.

Secondly, the simulation part of this study does not completely reflect the method of postprocessing in the clinical routine using Corridor4DM because it did not require a new segmentation of the myocardium for each temporal sampling protocol. However, it did show the effect of lesser time frames and provided us a selected number of temporal sampling protocols which we could validate. Furthermore, the simulation tool used a frame time weighting for the calculation of MBF while Corridor4DM uses a uniform weighting in the clinical routine. This might explain the differences in bias of the protocol with 20 and 14 frames between the simulation and validation study.

Thirdly, the validation part of this study required manual actions. These manual actions might have introduced operator-variability. For example, the occurrence of myocardial creep requires manual actions while detection and correction have to be performed manually [61]. This might also explain the high SD of the relative differences of $>10\%$ found for the RCA territory, as shown in Table 3, as myocardial creep primarily effects MBF quantification of the RCA territory. Furthermore, this

might also explain the differences observed between the SD of the relative differences for the global stress MBF of the simulation and validation study (20 frames: 3.0% vs 7.0% ; 14 frames: 4.5% vs 6.6%). Besides the variability introduced due to the use of different temporal sampling protocols, the validation study also contains operator-variability. However, the SD of the relative differences for global rest and stress MBF was still within the 10% methodological precision. It is likely that the variation due to only the temporal sampling protocol is therefore even lower than the ones reported in the validation part of this study.

Lastly, the minimal number of time frames tested in this study was 14. This protocol can be considered for clinical adoption while it had a methodological precision within 10%. It might even be possible to further decrease the number of time frames. Future research can be performed to test temporal sampling protocols with less than 14 frames until the methodological precision exceeds 10%.

There are several factors in the process of MBF quantification which affect the reliability of MBF measurement, using either 26 or 14 frames. During the process of MBF quantification we saw that the first step of defining the ROIs can have large effects on the MBF values if this is not performed adequately. Especially in patients with infarcted areas. We saw that it is hard to define the myocardium contours if there is hardly any activity visible due to an infarcted area. This likely introduced operator variability when comparing different temporal sampling protocols but even more important, results in unreliable MBF measurements if not performed adequately. Besides this step, detection and correction of myocardial creep also has to be performed. It is important that technologists who perform the quantification of MBF measurements are well trained so the operator variability is minimized and MBF measurements are reliable.

Furthermore, the simulation part of this study showed different absolute systemic biases in the global stress MBF between the temporal sampling protocols. This has to be taken into account in the detection of CAD. To maintain the same diagnostic accuracy among all centers performing MBF quantification using Rb-82 PET, it might be necessary to define cut off values according to the used protocol.

Conclusions

Considering our results and current literature, the last 240 seconds of the temporal sampling protocol can be sampled with frame durations of 120 seconds. Moreover, the minimal number of frames that still provides precise MBF measurements is 14. This protocol minimized the number of time frames and therefore reduces reconstruction time. This could provide the possibility for a “one-stop shop”. As the choice of temporal sampling protocol influences MBF outcomes, it might be necessary to define cut off values according to the used protocol.

Chapter 6

Future perspectives & general conclusion

Future perspectives

The studies described in this thesis show that correction of myocardial creep seems necessary to obtain reliable MBF measurements. Instructions on how to detect and correct this myocardial creep are also given. Furthermore, we have shown that the temporal sampling protocol used in the clinical routine can be minimized to 14 frames. This reduces reconstruction time and therefore could provide the possibility for a “one-stop shop”. This applies in particular to hospitals that do not have the newest computers and reconstruction time therefore takes a long time. As the choice of temporal sampling protocol influences MBF outcomes, it might be necessary to define cut off values according to the used protocol.

Although we made new steps in the optimization process of MBF quantification in Rb-82 PET, there are still topics which have to be assessed. The use of a patient specific dose instead of a fixed dose in Rb-82 PET MPI, which is already done for CZT-SPECT MPI, might standardize image quality [65].

Secondly, our study focused on Rb-82 PET. Although Rb-82 is widely available because it requires a generator instead of a cyclotron and has a short half-life, it has a low extraction and longer positron range which both decrease image quality [20]. Approval of the experimental PET radiopharmaceutical Flurpiridaz Fluor-18 (F-18) might enable improved clinical MPI with PET. It has a high myocardial retention, low background in adjacent organs and linear myocardial uptake throughout the range of flow [66, 67]. Therefore, this tracer might come close to an ideal myocardial perfusion tracer. Although this tracer seems promising, the half-life of Flurpiridaz F-18 is 108 minutes [22]. Extra rooms are required where patients can wait in case of a one-day protocol as the stress and rest scan cannot be acquired 10 minutes apart as is the case when using Rb-82. Furthermore, it might require an additional AC-CT scan while the patient moves off and on the scan table between the rest and stress scan. Therefore, the protocol used for Rb-82 has to be adjusted for Flurpiridaz F-18. Before any of this becomes reality, another phase III trial has to be performed to assess its value in clinical practice.

Thirdly, we see a lot of variability in the TACs in clinical practice. For example, we see a lot of variability in the first pass phase duration. The effect of variability in the first pass phase duration on MBF measurements is unknown and therefore, have to be assessed. It might give new insights in the reliability of MBF measurements.

Fourthly, we have shown the effect of myocardial creep on MBF quantification and the need of correcting for it during the post processing [61]. However, as myocardial creep occurs primarily during the earlier time frames, misregistration and, hence, attenuation correction artefacts may occur which can alter MBF quantification [57–60]. Frame-based co-registration of the stress-PET and CT data therefore might further improve PET/CT registration and thereby the reliability of Rb-82 PET quantification in patients with myocardial creep [53].

Furthermore, we did not find the minimum number of time frames resulting in a SD of the relative differences that exceeds the methodological precision of 10%. Therefore, temporal sampling protocols with less than 14 frames should be tested. Reconstruction time could even further decrease.

Despite the rapid growth of MBF quantification in PET MPI, a high variability in temporal sampling protocols exists between centers [33]. We showed that systemic biases differ between temporal sampling protocols. Therefore, it seems necessary that every center using MBF quantification should define its own cut off values or a standard protocol for all centers should be

used to maintain the diagnostic accuracy among all centers. Furthermore, other aspects which affect MBF quantification such as reconstruction method and tracer kinetic modeling also differ among centers [8]. Standardization of acquisition and reconstruction protocols would lower this variability and further optimize MBF quantification [14].

Lastly, defining the added clinical value in the management of patients with known or suspected CAD is important. Standardization would help to perform large studies in the future which can play a major role in determining the clinical added value of MBF quantification and increase the quality of its prognostic value. This helps to determine optimal management pathways for these patients.

Clinical implications

This thesis has several clinical implications considering the occurrence of myocardial creep and the minimization of the number of time frames. It is recommended to check for the presence of myocardial creep regardless of the used pharmacological vasodilator or used PET tracer. If myocardial creep remains uncorrected, this results in an overestimation of the stress MBF and MFR of especially the RCA territory [61]. This can lead to an incorrect diagnosis.

The presence of myocardial creep can be recognized by an elevated TAC of the RCA and a misalignment between the observed activity during the first pass phase and the myocardium contour. It is important that physicians always check for accurate myocardial creep correction before clinical interpretation.

Furthermore, the minimal number of 14 time frames tested in this study resulted in precise MBF measurements compared to the currently used temporal sampling protocol with 26 frames. This decrease in the number of time frames reduces reconstruction time of the dynamic series in Isala and other hospitals that do not have the newest computers. Using the temporal sampling protocol with 14 frames instead of the currently used 26 frames reduces the reconstruction time of the dynamic series from 32 minutes to 17 minutes and 16 seconds. Reconstruction of the static images takes 2 minutes and 54 seconds and reconstruction of the gated images takes 23 minutes 12 seconds. The total duration for reconstruction is therefore decreased from 58 minutes and 10 seconds to 43 minutes and 22 seconds. This reduction in reconstruction time could provide the possibility for a “one-stop shop”. A patient lies approximately 45 minutes on the scan table. Reconstructions of the previous patient can be finished within these 45 minutes using the protocol with 14 frames. In case of the currently reconstruction time, reconstructions have to be made after all patients are scanned otherwise it will cause a delay in the program.

General conclusion

The studies described in this thesis on further optimization of MBF quantification showed the impact of myocardial creep on MBF quantification and the minimal number of time frames that can be used. Myocardial creep occurred in more than half of the patients and significantly affects stress MBF and MFR quantification. Detection and correction of myocardial creep seem necessary to obtain accurate MBF measurements.

Furthermore, the temporal sampling protocol used in the clinical routine can be minimized to 14 frames. This reduces reconstruction time and therefore provides the possibility for a “one-stop shop”.

References

1. Buddeke J, Van Dis I, Visseren F, Vaartjes I, Bots M. Hart- en vaatziekten in Nederland 2017, cijfers over leefstijl, risicofactoren, ziekte en sterfte. Den Haag: Hartstichting, 2017.
2. Montalescot G, Sechtem U, Achenbach S, Andreotti F, Arden C, Budaj A, et al. 2013 ESC guidelines on the management of stable coronary artery disease. *Eur Heart J* 2013;34:2949–3003.
3. Ziadi MC, DeKemp RA, Williams K, Guo A, Renaud JM, Chow BJW, et al. Does quantification of myocardial flow reserve using rubidium-82 positron emission tomography facilitate detection of multivessel coronary artery disease? *J Nucl Cardiol* 2012;19:670–680.
4. Parkash R, deKemp RA, Ruddy TD, Kitsikis A, Hart R, Beauschene L, et al. Potential utility of rubidium 82 PET quantification in patients with 3-vessel coronary artery disease. *J Nucl Cardiol* 2004;11:440–449.
5. Santana CA, Folks RD, Garcia E V, Verdes L, Sanyal R, Hainer J, et al. Quantitative (82)Rb PET/CT: development and validation of myocardial perfusion database. *J Nucl Med* 2007;48:1122–1128.
6. Ziadi MC. Myocardial flow reserve (MFR) with positron emission tomography (PET)/computed tomography (CT): clinical impact in diagnosis and prognosis. *Cardiovasc Diagn Ther* 2017;7:206–218.
7. Lortie M, Beanlands RSB, Yoshinaga K, Klein R, DaSilva JN, DeKemp RA. Quantification of myocardial blood flow with 82Rb dynamic PET imaging. *Eur J Nucl Med Mol Imaging* 2007;34:1765–1774.
8. Moody JB, Lee BC, Corbett JR, Ficaro EP, Murthy VL. Precision and accuracy of clinical quantification of myocardial blood flow by dynamic PET: A technical perspective. *J Nucl Cardiol* 2015;22:935–951.
9. Koenders S. The intra- and inter-observer reproducibility for myocardial blood flow and coronary flow reserve quantification in time of flight 82Rubidium PET and the difference between time of flight and non-time of flight. 2017;report internship.
10. Dijk JD van, Jager PL, Dalen JA van. Pitfalls in myocardial blood flow quantification with rubidium-82 PET. *Tijdschr voor Nucl Geneesk* 2017;39:1822–1829.
11. Hansson GK. Inflammation, Atherosclerosis, and Coronary Artery Disease. *N Engl J Med* 2005;352:1685–1695.
12. Roffi M, Patrono C, Collet J-P, Mueller C, Valgimigli M, Andreotti F, et al. 2015 ESC Guidelines for the management of acute coronary syndromes in patients presenting without persistent ST-segment elevation. *Eur Heart J* 2016;37:267–315.
13. Rubin R, Strayer D, Rubin E. Ischemic Heart Disease. *Rubin's Pathol. Clin. Found. Med.*
14. van Dijk JD. Image quality and radiation dose in cardiac imaging. University of Twente
15. Johnson NP, Gould KL. Integrating noninvasive absolute flow, coronary flow reserve, and ischemic thresholds into a comprehensive map of physiological severity. *JACC Cardiovasc Imaging* 2012;5:430–440.
16. Jaarsma C, Leiner T, Bekkers SC, Crijns HJ, Wildberger JE, Nagel E, et al. Diagnostic Performance of Noninvasive Myocardial Perfusion Imaging Using Single-Photon Emission Computed Tomography, Cardiac Magnetic Resonance, and Positron Emission Tomography Imaging for the Detection of Obstructive Coronary Artery Disease: A Meta-Analysis. *J Am Coll Cardiol* 2012;59:1719–1728.
17. Votavová R, Linhartová A, Kořínek J, Marek J, Linhart A. Echocardiography in coronary artery disease. *Cor Vasa* 2015;57:e408–e418.
18. Mavrogeni S, Kolovou G. Role of cardiovascular magnetic resonance in interventional cardiology. *Contin Cardiol Educ* 2016;2:25–31.
19. Nakazato R, Berman DS, Alexanderson E, Slomka P. Myocardial perfusion imaging with PET. *Imaging Med* 2013;5:35–46.
20. Boyden TF, Murthy VL. Risk Stratification with Cardiac Rubidium-82 Positron Emission

- Tomography. *Curr Cardiovasc Imaging Rep* 2014;7:9266.
21. Johnson NP, Leonard SM, Gould KL. *Nuclear Cardiology: SPECT and PET*. Pract. Signal Image Process. Clin. Cardiol. Springer London, London, 2010; 219–250
 22. Maddahi J, Packard RRS. Cardiac PET perfusion tracers: current status and future directions. *Semin Nucl Med* 2014;44:333–343.
 23. Kaufmann PA, Camici PG. Myocardial Blood Flow Measurement by PET: Technical Aspects and Clinical Applications. *J Nucl Med* 2005;46:75–88.
 24. Klein R, Beanlands RSB, deKemp RA. Quantification of myocardial blood flow and flow reserve: Technical aspects. *J Nucl Cardiol* 2010;17:555–570.
 25. Iskandrian AE, Bateman TM, Belardinelli L, Blackburn B, Cerqueira MD, Hendel RC, et al. Adenosine versus regadenoson comparative evaluation in myocardial perfusion imaging: Results of the ADVANCE phase 3 multicenter international trial. *J Nucl Cardiol* 2007;14:645–658.
 26. Jager PL, Buiting M, Mouden M, Oostdijk AHJ, Timmer J, Knollema S. Regadenoson as a new stress agent in myocardial perfusion imaging. Initial experience in The Netherlands. *Rev Esp Med Nucl Imagen Mol* 2014;33:346–351.
 27. Cerqueira MD, Nguyen P, Staehr P, Underwood SR, Iskandrian AE. Effects of Age, Gender, Obesity, and Diabetes on the Efficacy and Safety of the Selective A2A Agonist Regadenoson Versus Adenosine in Myocardial Perfusion Imaging. Integrated ADVANCE-MPI Trial Results. *JACC Cardiovasc Imaging* 2008;1:307–316.
 28. Johnson SG, Peters S. Advances in Pharmacologic Stress Agents: Focus on Regadenoson. *J Nucl Med Technol* 2010;38:163–171.
 29. Belardinelli L, Shryock JC, Snowdy S, Zhang Y, Monopoli A, Lozza G, et al. The A2A adenosine receptor mediates coronary vasodilation. *J Pharmacol Exp Ther* 1998;284:1066–1073.
 30. Hendel RC, Bateman TM, Cerqueira MD, Iskandrian AE, Leppo JA, Blackburn B, et al. Initial clinical experience with regadenoson, a novel selective A 2A agonist for pharmacologic stress single-photon emission computed tomography myocardial perfusion imaging. *J Am Coll Cardiol* 2005;46:2069–2075.
 31. Saraste A, Kajander S, Han C, Nesterov S V., Knuuti J. PET: Is myocardial flow quantification a clinical reality? *J Nucl Cardiol* 2012;19:1044–1059.
 32. van Dijk JD, Huizing ED, van Dalen JA, Timmer JR, Jager PL. Minimal starting time of data reconstruction for qualitative myocardial perfusion rubidium-82 positron emission tomography imaging. *Nucl Med Commun* 2018;39:533–538.
 33. Klein R, Ocneanu A, deKemp RA. Time-frame sampling for 82Rb PET flow quantification: Towards standardization of clinical protocols. *J Nucl Cardiol* 2017;24:1530–1534.
 34. Lee BC, Moody JB, Weinberg RL, Corbett JR, Ficaro EP, Murthy VL. Optimization of temporal sampling for 82rubidium PET myocardial blood flow quantification. *J Nucl Cardiol* 2017;24:1517–1529.
 35. Murthy VL, Bateman TM, Beanlands RS, Berman DS, Borges-Neto S, Chareonthaitawee P, et al. Clinical Quantification of Myocardial Blood Flow Using PET: Joint Position Paper of the SNMMI Cardiovascular Council and the ASNC. *J Nucl Cardiol* 2018;25:269–297.
 36. Nesterov S V, Lee BC, Moody JB, Slomka P, Han C, Knuuti JM. The Status and Future of PET Myocardial Blood Flow Quantification Software. *Ann Nucl Cardiol* 2016;2:106–110.
 37. Hove J, Gambhir S, Kofoed K, Freiberg J, Kelbæk H. Quantitation of the regional blood flow in the interventricular septum using positron emission tomography and nitrogen-13 ammonia. *Eur J Nucl Med Mol Imaging* 2003;30:109–116.
 38. Hove JD, Iida H, Kofoed KF, Freiberg J, Holm S, Kelbaek H. Left atrial versus left ventricular input function for quantification of the myocardial blood flow with nitrogen-13 ammonia and positron emission tomography. *Eur J Nucl Med Mol Imaging* 2004;31:71–76.
 39. deKemp RA, Yoshinaga K, Beanlands RSB. Will 3-dimensional PET-CT enable the routine quantification of myocardial blood flow? *J Nucl Cardiol* 2007;14:380–397.
 40. Sciagrà R, Passeri A, Bucierius J, Verberne HJ, Slart RHJA, Lindner O, et al. Clinical use of quantitative cardiac perfusion PET: rationale, modalities and possible indications. Position

- paper of the Cardiovascular Committee of the European Association of Nuclear Medicine (EANM). *Eur J Nucl Med Mol Imaging* 2016;43:1530–1545.
41. Machac J. *Radiopharmaceuticals for Clinical Cardiac PET Imaging*. Card. PET PET/CT Imaging. Springer New York, New York, NY, 2007; 73–82
 42. Cerqueira MD, Verani MS, Schwaiger M, Heo J, Iskandrian AS. Safety profile of adenosine stress perfusion imaging: Results from the adenoscan multicenter trial registry. *J Am Coll Cardiol* 1994;23:384–389.
 43. Ranhosky A, Kempthorne-Rawson J. The safety of intravenous dipyridamole thallium myocardial perfusion imaging. Intravenous Dipyridamole Thallium Imaging Study Group. *Circulation* 1990;81:1205–1209.
 44. Cullom SJ, Case JA, Courter SA, McGhie AI, Bateman TM. Regadenoson pharmacologic rubidium-82 PET: A comparison of quantitative perfusion and function to dipyridamole. *J Nucl Cardiol* 2013;20:76–83.
 45. Hsiao E, Ali B, Blankstein R, Skali H, Ali T, Bruyere Jr. J, et al. Detection of Obstructive Coronary Artery Disease Using Regadenoson Stress and Rb-82 PET/CT Myocardial Perfusion Imaging. *J Nucl Med* 2013;54:1748–1754.
 46. Goudarzi B, Fukushima K, Bravo P, Merrill J, Bengel FM. Comparison of the myocardial blood flow response to regadenoson and dipyridamole: A quantitative analysis in patients referred for clinical 82Rb myocardial perfusion PET. *Eur J Nucl Med Mol Imaging* 2011;38:1908–1916.
 47. Memmott MJ, Tonge CM, Saint KJ, Arumugam P. Impact of pharmacological stress agent on patient motion during rubidium-82 myocardial perfusion PET/CT. *J Nucl Cardiol* 2017;1–10.
 48. Hunter CRRN, Klein R, Beanlands RS, DeKemp RA. Patient motion effects on the quantification of regional myocardial blood flow with dynamic PET imaging. *Med Phys* 2016;43:1829–1840.
 49. Koshino K, Watabe H, Enmi J, Hirano Y, Zeniya T, Hasegawa S, et al. Effects of patient movement on measurements of myocardial blood flow and viability in resting 15O-water PET studies. *J Nucl Cardiol* 2012;19:524–533.
 50. Piccinelli M, Votaw JR, Garcia E V. Motion Correction and Its Impact on Absolute Myocardial Blood Flow Measures with PET. *Curr Cardiol Rep* 2018;20:34.
 51. Friedman J, Van Train K, Maddahi J, Rozanski A, Prigent F, Bietendorf J, et al. Upward creep of the heart: a frequent source of false-positive reversible defects during thallium-201 stress-redistribution SPECT. *J Nucl Med* 1989;30:1718–1722.
 52. Votaw JR, Packard RRS. Technical aspects of acquiring and measuring myocardial blood flow: Method, technique, and QA. *J Nucl Cardiol* 2018;25:665–670.
 53. Lee BC, Moody JB, Poitrasson-Rivière A, Melvin AC, Weinberg RL, Corbett JR, et al. Blood pool and tissue phase patient motion effects on 82rubidium PET myocardial blood flow quantification. *J Nucl Cardiol* 2018;1–12.
 54. Karacalioglu AO, Jata B, Kilic S, Arslan N, Ilgan S, Ozguven MA. A physiologic approach to decreasing upward creep of the heart during myocardial perfusion imaging. *J Nucl Med Technol* 2006;34:215–219.
 55. van Dijk JD, van Dalen JA, Mouden M, Ottervanger JP, Knollema S, Slump CH, et al. Value of automatic patient motion detection and correction in myocardial perfusion imaging using a CZT-based SPECT camera. *J Nucl Cardiol* 2016;1–10.
 56. Kitkungvan D, Johnson NP, Roby AE, Patel MB, Kirkeeide R, Gould KL. Routine Clinical Quantitative Rest Stress Myocardial Perfusion for Managing Coronary Artery Disease: Clinical Relevance of Test-Retest Variability. *JACC Cardiovasc Imaging* 2017;10:565–577.
 57. Rajaram M, Tahari AK, Lee AH, Lodge MA, Tsui B, Nekolla S, et al. Cardiac PET/CT misregistration causes significant changes in estimated myocardial blood flow. *J Nucl Med* 2013;54:50–54.
 58. Martinez-Möller A, Souvatzoglou M, Navab N, Schwaiger M, Nekolla SG. Artifacts from misaligned CT in cardiac perfusion PET/CT studies: frequency, effects, and potential solutions. *J Nucl Med* 2007;48:188–193.
 59. Loghin C, Sdringola S, Gould KL. Common artifacts in PET myocardial perfusion images due to attenuation-emission misregistration: clinical significance, causes, and solutions. *J Nucl Med*

2004;45:1029–1039.

60. Gould KL, Pan T, Loghin C, Johnson NP, Guha A, Sdringola S. Frequent diagnostic errors in cardiac PET/CT due to misregistration of CT attenuation and emission PET images: a definitive analysis of causes, consequences, and corrections. *J Nucl Med* 2007;48:1112–1121.
61. Koenders SS, van Dijk JD, Jager PL, Ottervanger JP, Slump CH, van Dalen JA. Impact of regadenoson induced myocardial creep on dynamic Rubidium-82 PET myocardial blood flow quantification. *J Nucl Cardiol* 2018;In press.
62. Mateos-Pérez JM, Desco M, Vaquero JJ. Tracer Kinetic Modeling with R for Batch Processing of Dynamic PET Studies. Springer, Cham, 2014; 301–304
63. Dekemp RA, Declerck J, Klein R, Pan X-B, Nakazato R, Tonge C, et al. Multisoftware reproducibility study of stress and rest myocardial blood flow assessed with 3D dynamic PET/CT and a 1-tissue-compartment model of ^{82}Rb kinetics. *J Nucl Med* 2013;54:571–577.
64. Raylman RR, Caraher JM, Hutchins GD. Sampling requirements for dynamic cardiac PET studies using image-derived input functions. *J Nucl Med* 1993;34:440–447.
65. van Dijk JD, Jager PL, Mouden M, Slump CH, Ottervanger JP, de Boer J, et al. Development and validation of a patient-tailored dose regime in myocardial perfusion imaging using CZT-SPECT. *J Nucl Cardiol* 2014;21:1158–1167.
66. Maddahi J, Czernin J, Lazewatsky J, Huang S-C, Dahlbom M, Schelbert H, et al. Phase I, First-in-Human Study of BMS747158, a Novel ^{18}F -Labeled Tracer for Myocardial Perfusion PET: Dosimetry, Biodistribution, Safety, and Imaging Characteristics After a Single Injection at Rest. *J Nucl Med* 2011;52:1490–1498.
67. Berman DS, Maddahi J, Tamarappoo BK, Czernin J, Taillefer R, Udelson JE, et al. Phase II Safety and Clinical Comparison With Single-Photon Emission Computed Tomography Myocardial Perfusion Imaging for Detection of Coronary Artery Disease. *J Am Coll Cardiol* 2013;61:469–477.

